

Fig. 1. Plasma TAFI level for each age group of males and females. The graph shows age group means (columns) and SD (bars). \* $P < 0.05$ , \*\*  $P < 0.005$  male versus female.

Table 2b. Genotype distribution of the 202 normal subjects and plasma TAFI levels before and after 50 years of age

	Males		Females		Total	
	N; mean $\pm$ SD (mg/liter)		N; mean $\pm$ SD (mg/liter)		N; mean $\pm$ SD (mg/liter)	
	-50	51-	-50	51-	-50	51-
Thr147Ala						
Thr/Thr	3; 21.4 $\pm$ 4.46	3; 22.0 $\pm$ 5.87	8; 18.5 $\pm$ 2.25	3; 22.2 $\pm$ 5.06	11; 19.3 $\pm$ 3.06	6; 22.1 $\pm$ 4.90
Thr/Ala	33; 18.0 $\pm$ 3.81	11; 18.5 $\pm$ 2.79	33; 16.6 $\pm$ 3.66	17; 19.9 $\pm$ 4.67	66; 17.3 $\pm$ 3.78	28; 19.4 $\pm$ 4.04
Ala/Ala	12; 16.4 $\pm$ 3.53	11; 15.9 $\pm$ 3.84	46; 14.0 $\pm$ 2.70	22; 17.8 $\pm$ 3.34	58; 14.5 $\pm$ 3.02	33; 17.2 $\pm$ 3.56
Allele Thr	39 (40.6%)	17 (34.0%)	49 (28.2%)	23 (27.4%)	88 (32.6%)	40 (29.9%)
Allele Ala	57 (59.4%)	33 (66.0%)	125 (71.8%)	61 (72.6%)	182 (67.4%)	94 (70.1%)
Thr325Ile						
Thr/Thr	36; 18.9 $\pm$ 3.68	17; 18.9 $\pm$ 4.28	63; 16.0 $\pm$ 3.35	33; 19.6 $\pm$ 4.20	99; 17.1 $\pm$ 3.72	50; 19.4 $\pm$ 4.20
Thr/Ile	11; 14.6 $\pm$ 2.68	7; 15.8 $\pm$ 1.92	19; 14.2 $\pm$ 2.83	6; 16.5 $\pm$ 2.53	30; 14.4 $\pm$ 2.74	13; 16.1 $\pm$ 2.16
Ile/Ile	1; 12.7	1; 15.9	5; 12.1 $\pm$ 3.71	3; 16.3 $\pm$ 4.79	6; 12.7 $\pm$ 3.66	4; 15.4 $\pm$ 4.31
Allele Thr	83 (86.5%)	41 (82.0%)	145 (83.3%)	72 (85.7%)	228 (84.4%)	113 (84.3%)
Allele Ile	13 (13.5%)	9 (18.0%)	29 (16.7%)	12 (14.3%)	42 (15.6%)	21 (15.7%)

for each group did not deviate significantly from HWE. However, as shown in Table 1a and b, the difference between males and females was due to the male Ala/Ala-147 volunteers. Compared with our previous group of population-based aged controls (1) the  $P$  value in this report was 0.042 male Thr147Ala alleles in males. In this study, 73 males among the 202 normal

subjects were aged  $45.4 \pm 18.27$  while the remaining ranged from 20–93, and all were from central Japan. Our previous samples (1) were from an  $80.5 \pm 8.0$  year-old population from western Japan. This gap in age was not considered significant with respect to Thr147Ala alleles. In fact, as seen in Table 2b, the genotype distributions for those in the before and after

Table 2c. Statistical representation of the difference in the plasma TAFI levels of females with each genotype before and after 50 years of age

Thr147Ala	P value			P value			P value		
	-50			51-			-50 vs. 51-		
	Thr/Thr	Thr/Ala	Ala/Ala	Thr/Thr	Thr/Ala	Ala/Ala	Thr/Thr	Thr/Ala	Ala/Ala
Thr/Thr	/	-	-	/	-	-	/	-	0.11
Thr/Ala	0.17	/	-	0.45	/	-	0.085	/	0.0085
Ala/Ala	0.00005	0.0005	/	0.05	0.11	/	0.0000	/	0.0000

Thr325Ile	P value			P value			P value		
	-50			51-			-50 vs. 51-		
	Thr/Thr	Thr/Ile	Ile/Ile	Thr/Thr	Thr/Ile	Ile/Ile	Thr/Thr	Thr/Ile	Ile/Ile
Thr/Thr	/	-	-	/	-	-	/	-	0.00001
Thr/Ile	0.037	/	-	0.090	/	-	0.089	/	0.089
Ile/Ile	0.015	0.18	/	0.20	0.93	/	0.210	/	0.210

□ P < 0.05, ■ P < 0.005.

age 50 groups were not significantly different. Accordingly, any genotypic gap relative to Thr147Ala in normal males would reflect a regional difference. However, for males and females in general, the Thr147Ala distributions presented previously by us (1) and others (8) were not significantly different from that of the present report.

In contrast, in the present study as in our previous report (1), findings regarding Thr325Ile, allele frequencies differed significantly from those of other investigators (8, 24).

This difference in allele frequencies at position 325 might simply be due to a racial difference between Caucasians and Japanese. In addition, some of the samples in our previous report were from subjects older than 80 years (1), and it is possible that the deviation observed in that study might have reflected the longer life span of our patients.

However, the average age of subjects in our previous report was around 60 years, while in other studies, it was around 50 (8, 21). The genotypic distribution of our Japanese subjects would also be expected to differ from that of Caucasians.

#### Plasma TAFI Level with Age for Each Genotype

It is obvious that plasma TAFI levels and activity are influenced by SNPs (20, 38). Although it cannot be seen clearly in Fig. 2, Table 1b shows a significant correlation between the plasma TAFI level and genotype. Among Thr147Ala and Thr325Ile polymorphisms, subjects with the Thr/Thr type had the highest TAFI level. On comparing males and females, male levels seemed higher but there was no statistical significance to this difference unless Thr/Thr at Thr325Ile was included. Our anti-proCPR-specific (anti-TAFI) monoclonal ELISA system also detected SNP differences.

In terms of age dependence, the TAFI level was down-regulated in the group of younger females, as seen in Fig. 1. In addition, this tendency was noted in each genetic type (Fig. 2b and d).

To clarify the data, the female plasma TAFI level was analyzed according to decade, and a statistically significant difference was detected between the 51-70 vs. 21-50 groups (Table 2b and c). The TAFI antigen level could be influenced by hormonal status and may reflect menopausal changes, as reported by Chetaille et al. (12).

All data were separated according to genotype into before and after age 50 groups and no significant difference was found in their genetic distribution. However, in each SNP group, the TAFI plasma level of the younger subjects (younger than age 50) differed significantly.

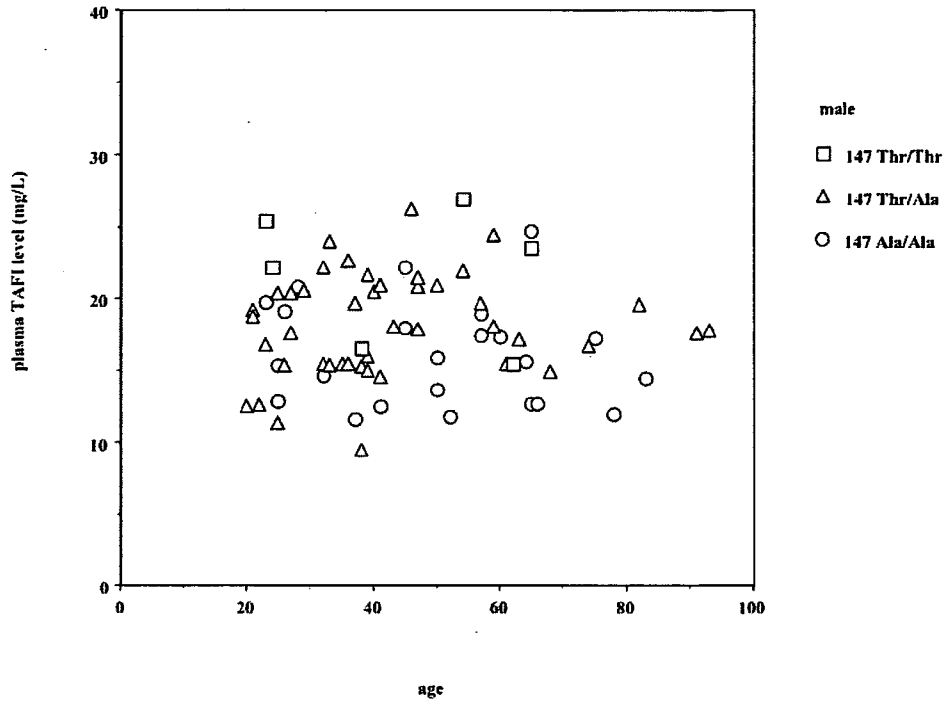
In subjects with the Thr/Ala and Ala/Ala alleles of Thr147Ala, the proCPR levels in the before versus the after age 50 groups were significantly different (Table 2c). For those who were 51 or older, the P value for Thr/Thr versus Ala/Ala was only 0.05. On the other hand, in those under 50, the Ala/Ala group deviated significantly from the Thr/Thr and Thr/Ala groups with regard to the plasma TAFI level (Table 2c).

This tendency was also observed with Thr325Ile. In this study, the Thr/Thr deviation was strongly significant. There was also a significant difference between this polymorphism and Thr/Ile and Ile/Ile, but only in the under-50 group.

In conclusion, the Ala/Ala at 147 and Ile/Ile at 325 group showed a tendency toward low levels of plasma proCPR (TAFI). However, in females, this tendency disappeared at around 50 years of age, suggesting a strong association with the onset of menopause.

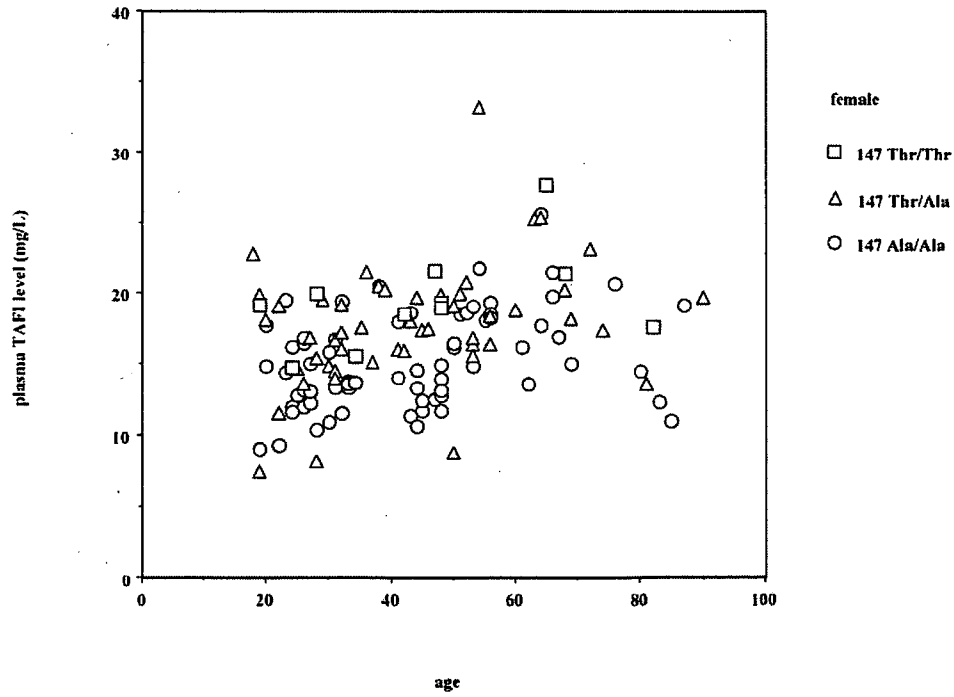
Before menopause, normal women experience a

(a)



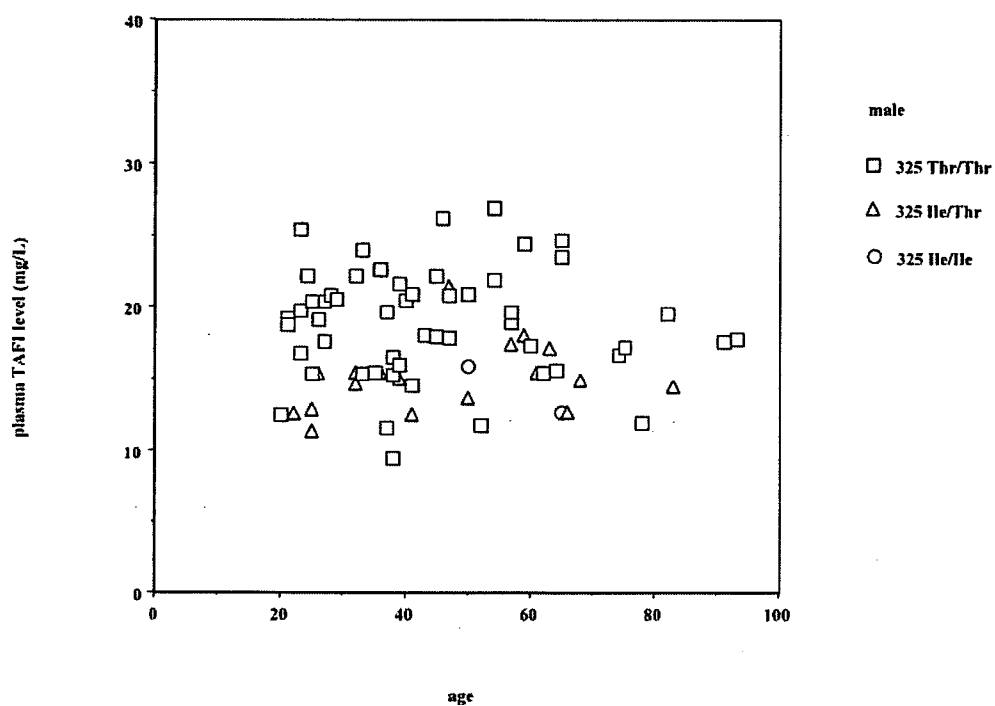
a

(b)



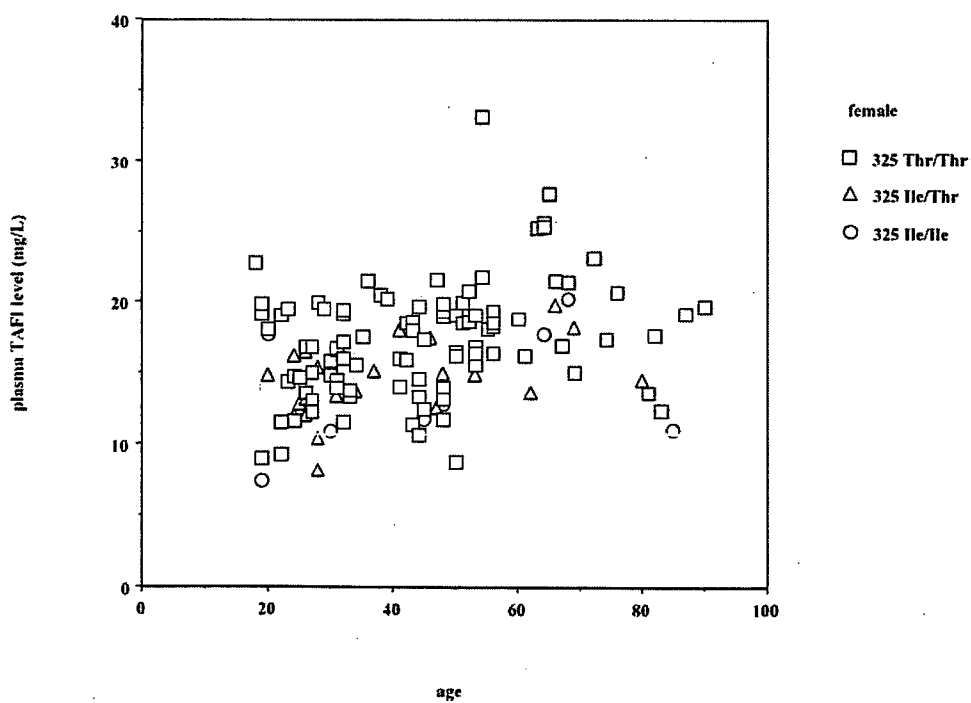
b

(c)



c

(d)



d

Fig. 2. Plasma TAFI level in males and females correlated with Thr147Ala and Thr325Ile genotypes. a: male Thr147Ala, b: female Thr147Ala. □ 147 Thr/Thr, △ 147 Thr/Ala, ○ 147 Ala/Ala. c: male Thr325Ile, d: female Thr325Ile. □ 325 Thr/Thr, △ 325 Ile/Thr, ○ 325 Ile/Ile. Each spot represents an individual.

monthly estradiol/progesterone menstrual cycle. Estradiol might be a particular candidate for reducing TAFI levels since oral estradiol/trimegestone replacement reduces TAFI production in early postmenopausal women (28) and 3 months of raloxifene treatment was associated with a significant decrease in the plasma TAFI antigen concentration (27). However, another study dismissed the short-term effects of estrogen, tamoxifen and raloxifene on the plasma TAFI level (13). Moreover, the TAFI level changes throughout a normal pregnancy, suggesting that it must correspond to hormonal fluctuations occurring during gestation.

Little is known of the biochemical mechanism underlying the hormonal effect on TAFI levels, especially in individuals with Ala/Ala at 147 or Thr/Thr at 325. However, as with the immunological response, lipopolysaccharide is likely a trigger (31). Molecular analysis of the human TAFI promoter region shows that the CCAAT/enhancer-binding protein (C/EBP)-binding site occupies positions -53 and -40 (5) and the functional glucocorticoid response element (GRE) occupies positions -92 and -78 (6). This suggests that TAFI is not only an acute phase protein but also regulates steroid hormones.

#### *Comparison of Plasma TAFI Levels and Other Biochemical Data*

Plasma TAFI is generated in liver (14) and platelets (25), and is up-regulated in acute inflammatory states (31). The concentration of TM is an important factor in the regulation of TAFI activation as well as in the regulation of fibrinolysis. High TM concentrations result in down-regulation of fibrinolysis, whereas low TM concentrations result in up-regulation (26). The thrombin-thrombomodulin complex (T/TM), rather than free thrombin, is the most likely physiological activator of TAFI (3).

However, under normal conditions, TAFI levels showed no correlation with platelets, with the liver enzymes AST and ALT, with the WBC count as an inflammatory marker, or with TM as a regulator of TAFI activation (data not shown).

In previous reports, the risk of acute coronary artery disease was associated with a disturbance in functional thrombin activatable fibrinolysis inhibitor plasma levels (30) as was the risk of deep vein thrombosis (39). Obstructive vascular disease as well as inflammatory states, burns and septic injuries induce profound changes in the coagulation status. In a rat model of burn and septic injury, TAFI levels increased significantly at 24- and 72-hr time points following burn, caecal ligation and puncture (CLP), and burn + CLP (29). In addition, TAFI mRNA was found to be up-regulated

in an LPS model (31). In contrast, Watanabe et al. measured plasma levels of TAFI antigen and activity in patients with disseminated intravascular coagulation (DIC) to examine the relationship between hypofibrinolysis and the pathogenesis of DIC and found that TAFI levels and activity in plasma were significantly low in these patients (40).

This was not a multi-center project, and our samples were limited to the patients and volunteers of a single hospital. Nevertheless, we were able to establish the normal plasma proCPR (TAFI) level taking age and Thr147Ala and Thr325Ile status into account. Because of variation in the geographical origin of our subjects, there was some deviation at Thr147Ala. However, considering genetics and age, a level of about 8–25 mg/liter was established as normal and not to reflect the influence of other factors. In future studies using these data, we will analyze the relationship between plasma proCPR (TAFI) levels and several thrombotic and inflammatory conditions.

We received support for this study from the Research Grants for the Future Program, Japan Society for the Promotion of Science (JSPS). We thank the patients and their guardians for cooperating with our project. We also thank Ms. Catherine Campbell for her help in editing this manuscript.

#### **References**

- 1) Akatsu, H., Yamagata, H., Chen, Y., Miki, T., Kamino, K., Takeda, M., Campbell, W., Kondo, I., Kosaka, K., Yamamoto, T., and Okada, H. 2004. TAFI polymorphisms at amino acids 147 and 325 are not risk factors for cerebral infarction. *Br. J. Haematol.* **127**: 440–447.
- 2) Bajzar, L., Manuel, R., and Nesheim, M.E. 1995. Purification and characterization of TAFI, a thrombin-activable fibrinolysis inhibitor. *J. Biol. Chem.* **270**: 14477–14484.
- 3) Bajzar, L., Morser, J., and Nesheim, M. 1996. TAFI, or plasma procarboxypeptidase B, couples the coagulation and fibrinolytic cascades through the thrombin-thrombomodulin complex. *J. Biol. Chem.* **271**: 16603–16608.
- 4) Belew, M., Gerdin, B., Lindeberg, G., Porath, J., Saldeen, T., and Wallin, R. 1980. Structure-activity relationships of vasoactive peptides derived from fibrin or fibrinogen degraded by plasmin. *Biochim. Biophys. Acta* **621**: 169–178.
- 5) Boffa, M.B., Hamill, J.D., Bastajian, N., Dillon, R., Nesheim, M.E., and Koschinsky, M.L. 2002. A role for CCAAT/enhancer-binding protein in hepatic expression of thrombin-activable fibrinolysis inhibitor. *J. Biol. Chem.* **277**: 25329–25336.
- 6) Boffa, M.B., Hamill, J.D., Maret, D., Brown, D., Scott, M.L., Nesheim, M.E., and Koschinsky, M.L. 2003. Acute phase mediators modulate thrombin-activable fibrinolysis inhibitor (TAFI) gene expression in HepG2 cells. *J. Biol. Chem.* **278**: 9250–9257.

- 7) Bokisch, V.A., and Muller-Eberhard, H.J. 1970. Anaphylatoxin inactivator of human plasma: its isolation and characterization as a carboxypeptidase. *J. Clin. Invest.* **49**: 2427–2436.
- 8) Brouwers, G.J., Vos, H.L., Leebeek, F.W., Bulk, S., Schneider, M., Boffa, M., Koschinsky, M., van Tilburg, N.H., Nesheim, M.E., Bertina, R.M., and Gomez Garcia, E.B. 2001. A novel, possibly functional, single nucleotide polymorphism in the coding region of the thrombin-activatable fibrinolysis inhibitor (TAFI) gene is also associated with TAFI levels. *Blood* **98**: 1992–1993.
- 9) Campbell, W., and Okada, H. 1989. An arginine specific carboxypeptidase generated in blood during coagulation or inflammation which is unrelated to carboxypeptidase N or its subunits. *Biochem. Biophys. Res. Commun.* **162**: 933–939.
- 10) Campbell, W., Yonezu, K., Shinohara, T., and Okada, H. 1990. An arginine carboxypeptidase generated during coagulation is diminished or absent in patients with rheumatoid arthritis. *J. Lab. Clin. Med.* **115**: 610–612.
- 11) Campbell, W.D., Lazoura, E., Okada, N., and Okada, H. 2002. Inactivation of C3a and C5a octapeptides by carboxypeptidase R and carboxypeptidase N. *Microbiol. Immunol.* **46**: 131–134.
- 12) Chetaille, P., Alessi, M.C., Kouassi, D., Morange, P.E., and Juhan-Vague, I. 2000. Plasma TAFI antigen variations in healthy subjects. *Thromb. Haemost.* **83**: 902–905.
- 13) Cosman, F., Baz-Hecht, M., Cushman, M., Vardy, M.D., Cruz, J.D., Nieves, J.W., Zion, M., and Lindsay, R. 2005. Short-term effects of estrogen, tamoxifen and raloxifene on hemostasis: a randomized-controlled study and review of the literature. *Thromb. Res.* **116**: 1–13.
- 14) Eaton, D.L., Malloy, B.E., Tsai, S.P., Henzel, W., and Drayna, D. 1991. Isolation, molecular cloning, and partial characterization of a novel carboxypeptidase B from human plasma. *J. Biol. Chem.* **266**: 21833–21838.
- 15) Erdos, E.G., and Sloane, E.M. 1962. An enzyme in human blood plasma that inactivates bradykinin and kallidins. *Biochem. Pharmacol.* **11**: 585–592.
- 16) Franco, R.F., Fagundes, M.G., Meijers, J.C., Reitsma, P.H., Lourenco, D., Morelli, V., Maffei, F.H., Ferrari, I.C., Piccinato, C.E., Silva, W.A., Jr., and Zago, M.A. 2001. Identification of polymorphisms in the 5'-untranslated region of the TAFI gene: relationship with plasma TAFI levels and risk of venous thrombosis. *Haematologica* **86**: 510–517.
- 17) Guimaraes, A.H., van Tilburg, N.H., Vos, H.L., Bertina, R.M., and Rijken, D.C. 2004. Association between thrombin activatable fibrinolysis inhibitor genotype and levels in plasma: comparison of different assays. *Br. J. Haematol.* **124**: 659–665.
- 18) Hendriks, D., Scharpe, S., van Sande, M., and Lommaert, M.P. 1989. Characterisation of a carboxypeptidase in human serum distinct from carboxypeptidase N. *J. Clin. Chem. Clin. Biochem.* **27**: 277–285.
- 19) Hendriks, D., Wang, W., Scharpe, S., Lommaert, M.P., and van Sande, M. 1990. Purification and characterization of a new arginine carboxypeptidase in human serum. *Biochim. Biophys. Acta* **1034**: 86–92.
- 20) Henry, M., Aubert, H., Morange, P.E., Nanni, I., Alessi, M.C., Tiret, L., and Juhan-Vague, I. 2001. Identification of polymorphisms in the promoter and the 3' region of the TAFI gene: evidence that plasma TAFI antigen levels are strongly genetically controlled. *Blood* **97**: 2053–2058.
- 21) Juhan-Vague, I., Morange, P.E., Aubert, H., Henry, M., Aillaud, M.F., Alessi, M.C., Samnegard, A., Hawe, E., Yudkin, J., Margaglione, M., Di Minno, G., Hamsten, A., and Humphries, S.E. 2002. Plasma thrombin-activatable fibrinolysis inhibitor antigen concentration and genotype in relation to myocardial infarction in the north and south of Europe. *Arterioscler. Thromb. Vasc. Biol.* **22**: 867–873.
- 22) Juhan-Vague, I., Renucci, J.F., Grimaux, M., Morange, P.E., Gouvernet, J., Gourmelin, Y., and Alessi, M.C. 2000. Thrombin-activatable fibrinolysis inhibitor antigen levels and cardiovascular risk factors. *Arterioscler. Thromb. Vasc. Biol.* **20**: 2156–2161.
- 23) Kostka, H., Kuhlisch, E., Schellong, S., and Siegert, G. 2003. Polymorphisms in the TAFI gene and the risk of venous thrombosis. *Clin. Lab.* **49**: 645–647.
- 24) Morange, P.E., Henry, M., Frere, C., and Juhan-Vague, I. 2002. Thr325Ile polymorphism of the TAFI gene does not influence the risk of myocardial infarction. *Blood* **99**: 1878–1879.
- 25) Mosnier, L.O., Buijtenhuijs, P., Marx, P.F., Meijers, J.C., and Bouma, B.N. 2003. Identification of thrombin activatable fibrinolysis inhibitor (TAFI) in human platelets. *Blood* **101**: 4844–4846.
- 26) Mosnier, L.O., Meijers, J.C., and Bouma, B.N. 2001. Regulation of fibrinolysis in plasma by TAFI and protein C is dependent on the concentration of thrombomodulin. *Thromb. Haemost.* **85**: 5–11.
- 27) Ozeren, M., Karahan, S.C., Ozgur, M., Eminagaoglu, S., Unsal, M., Baytan, S., and Bozkaya, H. 2005. The effects of short-term raloxifene therapy on fibrinolysis markers: TAFI, tPA, and PAI-1. *Acta Obstet. Gynecol. Scand.* **84**: 987–991.
- 28) Post, M.S., Hendriks, D.F., Van Der Mooren, M.J., Van Baal, W.M., Leurs, J.R., Emeis, J.J., Kenemans, P., and Stehouwer, C.D. 2002. Oral oestradiol/trimegestone replacement reduces procarboxypeptidase U (TAFI): a randomized, placebo-controlled, 12-week study in early postmenopausal women. *J. Intern. Med.* **251**: 245–251.
- 29) Ravindranath, T.M., Gotô, M., Demir, M., Tobu, M., Kujawski, M.F., Hoppensteadt, D., Samonte, V., Iqbal, O., Sayeed, M.M., and Fareed, J. 2004. Tissue factor pathway inhibitor and thrombin activatable fibrinolytic inhibitor plasma levels following burn and septic injuries in rats. *Clin. Appl. Thromb. Hemost.* **10**: 379–385.
- 30) Santamaria, A., Martinez-Rubio, A., Borrell, M., Mateo, J., Ortin, R., and Fontcuberta, J. 2004. Risk of acute coronary artery disease associated with functional thrombin activatable fibrinolysis inhibitor plasma level. *Haematologica* **89**: 880–881.
- 31) Sato, T., Miwa, T., Akatsu, H., Matsukawa, N., Obata, K., Okada, N., Campbell, W., and Okada, H. 2000. Pro-carboxypeptidase R is an acute phase protein in the mouse, whereas carboxypeptidase N is not. *J. Immunol.* **165**: 1053–1058.
- 32) Schneider, M., Boffa, M., Stewart, R., Rahman, M.,

- Koschinsky, M., and Nesheim, M. 2002. Two naturally occurring variants of TAFI (Thr-325 and Ile-325) differ substantially with respect to thermal stability and antifibrinolytic activity of the enzyme. *J. Biol. Chem.* **277**: 1021–1030.
- 33) Schroeder, V., Chatterjee, T., Mehta, H., Windecker, S., Pham, T., Devantay, N., Meier, B., and Kohler, H.P. 2002. Thrombin activatable fibrinolysis inhibitor (TAFI) levels in patients with coronary artery disease investigated by angiography. *Thromb. Haemost.* **88**: 1020–1025.
- 34) Shinohara, T., Sakurada, C., Suzuki, T., Takeuchi, O., Campbell, W., Ikeda, S., Okada, N., and Okada, H. 1994. Pro-carboxypeptidase R cleaves bradykinin following activation. *Int. Arch. Allergy Immunol.* **103**: 400–404.
- 35) Silveira, A., Schatteman, K., Goossens, F., Moor, E., Scharpe, S., Stromqvist, M., Hendriks, D., and Hamsten, A. 2000. Plasma procarboxypeptidase U in men with symptomatic coronary artery disease. *Thromb. Haemost.* **84**: 364–368.
- 36) Tani, S., Akatsu, H., Ishikawa, Y., Okada, N., and Okada, H. 2003. Preferential detection of pro-carboxypeptidase R by enzyme-linked immunosorbent assay. *Microbiol. Immunol.* **47**: 295–300.
- 37) Teger-Nilsson, A.C. 1968. Degradation of human fibrinopeptides A and B in blood serum *in vitro*. *Acta Chem. Scand.* **22**: 3171–3182.
- 38) Tregouet, D.A., Aubert, H., Henry, M., Morange, P., Visvikis, S., Juhan-Vague, I., and Tiret, L. 2001. Combined segregation-linkage analysis of plasma thrombin activatable fibrinolysis inhibitor (TAFI) antigen levels with TAFI gene polymorphisms. *Hum. Genet.* **109**: 191–197.
- 39) van Tilburg, N.H., Rosendaal, F.R., and Bertina, R.M. 2000. Thrombin activatable fibrinolysis inhibitor and the risk for deep vein thrombosis. *Blood* **95**: 2855–2859.
- 40) Watanabe, R., Wada, H., Watanabe, Y., Sakakura, M., Nakasaki, T., Mori, Y., Nishikawa, M., Gabazza, E.C., Nobori, T., and Shiku, H. 2001. Activity and antigen levels of thrombin-activatable fibrinolysis inhibitor in plasma of patients with disseminated intravascular coagulation. *Thromb. Res.* **104**: 1–6.
- 41) Zhao, L., Morser, J., Bajzar, L., Nesheim, M., and Nagashima, M. 1998. Identification and characterization of two thrombin-activatable fibrinolysis inhibitor isoforms. *Thromb. Haemost.* **80**: 949–955.
- 42) Zorio, E., Castello, R., Falco, C., Espana, F., Osa, A., Almenar, L., Aznar, J., and Estelles, A. 2003. Thrombin-activatable fibrinolysis inhibitor in young patients with myocardial infarction and its relationship with the fibrinolytic function and the protein C system. *Br. J. Haematol.* **122**: 958–965.

## Reduced Neuron-Specific Expression of the *TAF1* Gene Is Associated with X-Linked Dystonia-Parkinsonism

Satoshi Makino, Ryuji Kaji, Satoshi Ando, Maiko Tomizawa, Katsuhito Yasuno, Satoshi Goto, Shinnichi Matsumoto, Ma. Daisy Tabuena, Elma Maranon, Marita Dantes, Lillian V. Lee, Kazumasa Ogasawara, Ikuo Tooyama, Hiroyasu Akatsu, Masataka Nishimura, and Gen Tamiya

X-linked dystonia-parkinsonism (XDP) is a movement disorder endemic to the Philippines. The disease locus, *DYT3*, has been mapped to Xq13.1. In a search for the causative gene, we performed genomic sequencing analysis, followed by expression analysis of XDP brain tissues. We found a disease-specific SVA (short interspersed nuclear element, variable number of tandem repeats, and Alu composite) retrotransposon insertion in an intron of the TATA-binding protein-associated factor 1 gene (*TAF1*), which encodes the largest component of the TFIID complex, and significantly decreased expression levels of *TAF1* and the dopamine receptor *D2* gene (*DRD2*) in the caudate nucleus. We also identified an abnormal pattern of DNA methylation in the retrotransposon in the genome from the patient's caudate, which could account for decreased expression of *TAF1*. Our findings suggest that the reduced neuron-specific expression of the *TAF1* gene is associated with XDP.

X-linked dystonia-parkinsonism (XDP [MIM314250]) is characterized by severe progressive torsion dystonia followed by parkinsonism.<sup>1</sup> Its prevalence is high (5.24 in 100,000) on Panay Island, Philippines.<sup>2</sup> Dystonia is a syndrome of sustained muscle contractions causing twisting and repetitive movements or abnormal postures,<sup>3</sup> and its pathogenetic basis is still unclear. XDP has a well-defined pathology of extensive neuronal loss and mosaic gliosis in the striatum (caudate nucleus and putamen),<sup>4,5</sup> which appears to resemble that in Huntington disease (MIM 143100). Identification of the disease gene of XDP may contribute to the elucidation of the molecular basis underlying not only XDP itself but also other diseases in which basal ganglia show neurodegeneration, such as Huntington disease and Parkinson disease.

A series of linkage analyses has mapped the disease locus, *DYT3*, to Xq13.1 (fig. 1).<sup>6,7</sup> A linkage disequilibrium study narrowed the *DYT3* locus to within a 350-kb interval on Xq13.1.<sup>8</sup> Subsequently, Nolte et al.<sup>9</sup> used PCR-based sequencing and screening analyses to report four SNPs and five disease-specific sequence changes (DSCs) in the "multiple transcript system" (*MTS*) within 260 kb of the *DYT3* region. However, PCR often fails to detect large sequence variants such as transposons. Moreover, the previous study of *MTS* did not include any brain specimens from patients with XDP. Therefore, the structure and expression of *MTS* transcripts are still unclear.

We performed the following studies to reveal the dis-

ease-causative gene of XDP. To find all disease-specific mutations within the *DYT3* region, we first performed genomic sequencing analysis to accurately determine the complete DNA sequence of this region. We also performed detailed expression analysis of the gene in brain specimens obtained from patients with XDP, because the expression of disease genes can be tissue specific. To determine the complete structure of the disease gene, we used a library consisting of "full-length" cDNAs frequently containing their 5' ends.<sup>10</sup>

### Material and Methods

#### Subjects and Samples

The study included 67 Filipino individuals (20 affected males) from 16 families residing in Panay. Information on all the patients is listed in table 1. All patients had the disease-specific haplotype between *DXS10017* and *DXS10018* in the *DYT3* region that had been defined elsewhere.<sup>8,9</sup> For construction of the BAC contig and portions of the RNA analysis, lymphoblastoid cells were immortalized by infection with the Epstein-Barr virus. This study involved a total of 137 healthy control subjects: 14 unrelated Filipinos, 44 Japanese, 38 African Americans, and 43 European Americans. Materials from the non-Filipino individuals were commercially provided by Coriell Cell Repositories. We used seven postmortem brains from seven male Filipino patients who had XDP. One of the seven brain specimens was frozen, and six were formalin fixed immediately at autopsy. The information on these seven patients with XDP is provided in table 2. We used the frozen brain from a single patient with XDP for long RT-PCR,

From the Department of Neurology and Neuroscience, University of Tokushima Graduate School of Medicine, Tokushima, Japan (S. Makino; R.K.; S.A.; S. Matsumoto; M.N.; G.T.); Department of Molecular Life Science, Tokai University School of Medicine, Kanagawa, Japan (S. Makino; S.A.; M.T.; K.Y.; G.T.); Department of Neurosurgery, Graduate School of Medical Sciences, Kumamoto University, Kumamoto, Japan (S.G.); Department of Internal Medicine, Section of Neurology, West Visayas State University Medical Center, Jaro, Iloilo, Panay, Philippines (M.D.T.; E.M.); Department of Health, Philippine Children's Medical Center, Quezon City, Philippines (M.D.; L.V.L.); Department of Pathology (K.O.) and Molecular Neuroscience Research Center (I.T.), Shiga University of Medical Science, Otsu, Japan; and Choju Medical Institute, Fukushima Hospital, Toyohashi, Japan (H.A.)

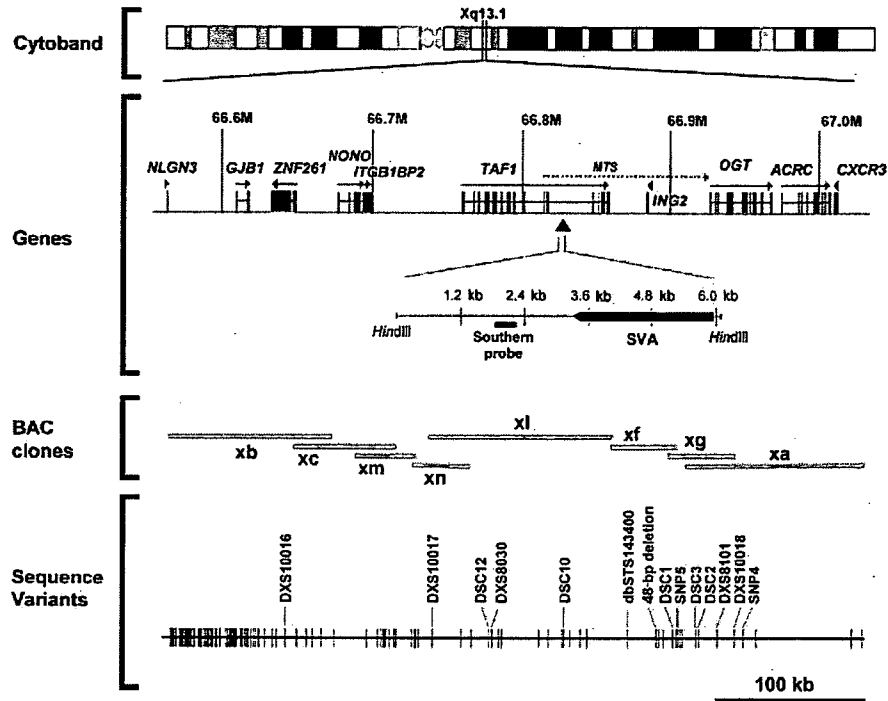
Received August 21, 2006; accepted for publication December 13, 2006; electronically published January 23, 2007.

Address for correspondence and reprints: Dr. Gen Tamiya, Department of Neurology and Neuroscience, University of Tokushima Graduate School of Medicine, Tokushima 770-8503, Japan. E-mail: gtamiya@genetix-h.com

*Am. J. Hum. Genet.* 2007;80:393–406. © 2007 by The American Society of Human Genetics. All rights reserved. 0002-9297/2007/8003-0002\$15.00  
DOI: 10.1086/512129



**a**



**b**

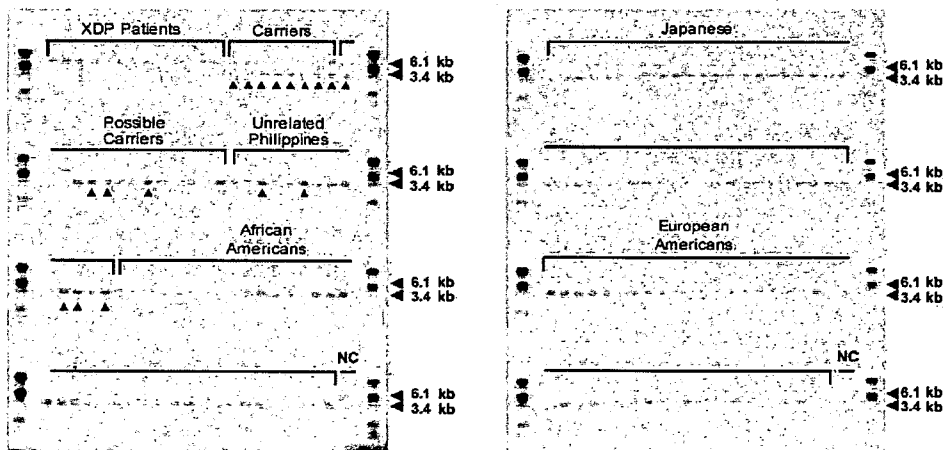


**Figure 1.** Genomic sequencing analysis of the *DYT3* region. *a*, Physical map of the *DYT3* critical region on Xq13.1. Annotated genes in this region that have experimentally verified coding sequences (and their proteins) include *NLGN3* (neuroligin 3), *GJB1* (gap junction protein, beta-1), *ZNF261* (zinc finger protein 261), *NONO* (non-POU domain-containing octamer-binding protein), *ITGB1BP2* (melusin [integrin beta-1 binding protein 2]), *TAF1* (TAF-250 [TATA-binding protein-associated factor, 250 kDa]), *ING2* (inhibitor of growth 2), *OGT* (O-linked N-acetylglucosamine transferase), *ACRC* (acid repeat-containing gene), and *CXCR3* (chemokine, CXC motif, receptor 3). The broken arrow indicates *MTS*. A unique Southern probe was designed for the *HindIII*-digested fragment containing the SVA retrotransposon insertion. Eight BAC clones comprising a continuous contig map cover 462,651 bp, from 66572462 to 67035112 in NCBI build 30. A total sequence length of 463,567 bp was determined, with 5.7-fold redundancy. Also shown is the distribution of 159 nucleotide variants that were identified by sequencing. None of these variants is located in any exon of these genes, including their alternative splicing forms. A red arrowhead indicates the SVA insertion. *b*, The SVA insertion in the XDP-related and healthy control populations. Information on the patients with XDP is given in table 1 (patients 1-13). The SVA insertion produces a 6.1-kb fragment, whereas the wild type produces a 3.4-kb fragment. Arrowheads in the gel indicate female individuals. Carriers are defined as mothers or daughters of patients with XDP. Possible carriers are daughters or sons of these carriers. NC = negative control.

**Table 1. Information on All the Patients with XDP Who Were Studied by Southern Hybridization**

Patient Number	Sample	Signal		Age at Onset (years)	Clinical Description
		6 kb	3 kb		
1	XD001	+	-	31	Generalized dystonia
2	XD002	+	-	38	Generalized dystonia
3	XD011	+	-	29	Muscle atrophy and generalized dystonia
4	XD013	+	-	45	No atrophy and dystonia
5	XD015	+	-	31	Limb atrophy and parkinsonism
6	XD024	+	-	41	Dystonia and parkinsonism
7	XD027	+	-	30	Dystonia and parkinsonism
8	XD028	+	-	30	Leg tremor and generalized dystonia
9	XD033	+	-	33	Parkinsonism (hand tremor)
10	XD036	+	-	50	Mild dystonia and parkinsonism
11	XD041	+	-	52	Dystonia and parkinsonism
12	XD054	+	-	30	Generalized dystonia
13	XD062	+	-	40	Severe atrophy
14	XD101	+	-	42	Swelling feet, difficulty walking, and sensory trick
15	XD103	+	-	46	Dystonia, parkinsonism, difficulty swallowing, and freezing gait
16	XD111	+	-	39	Dystonia, parkinsonism, and difficulty walking
17	XD112	+	-	33	Torticollis and parkinsonism
18	XD115	+	-	31	Jaw-opening dystonia and parkinsonism
19	XD131	+	-	36	Blepharospasm and writer's clamp
20	XD141	+	-	40	Cervical dystonia, axial dystonia, and parkinsonism

NOTE.—All patients are male. Plus sign (+) = presence of signal; minus sign (-) = absence of signal.

northern analysis, quantitative RT-PCR, and in situ hybridization. In addition, we used the six formalin-fixed brain specimens for immunohistochemical staining. This study complied with the ethical guidelines of the institutions involved.

#### Genome Analysis

We constructed two series of BAC libraries, using genomic DNA from a patient with XDP who was aged 41 years and had generalized torsion dystonia without parkinsonism. Cultured lymphoblastoid cells from a patient with XDP were embedded in agarose plugs, and then high-molecular-weight DNA was partially digested with *EcoRI* and was size fractionated by pulse-field gel electrophoresis. Size-fractionated DNA was cloned into the CopyControl pCC1BAC vector (Epicentre) and was transformed into DH10B cells by use of an electroporator. The same procedure was repeated with *HindIII*. We identified BACs covering the *DYT3* region by hybridizing <sup>32</sup>P-labeled PCR probes to filters generated from these BAC libraries. A shotgun library in pUC118 was con-

structed from each BAC clone. Cycle sequencing was performed using a BigDye Terminator v3.1 Cycle Sequencing kit (Applied Biosystems) and was analyzed on an ABI 3700 capillary sequencer. The gap clones were sequenced using a GPS-1 Genome Priming System (New England Biolabs). Raw sequence data were analyzed and assembled by ATGC software (Genetyx).

We digested 4 μg of genomic DNA in 300 μl of a standard reaction mixture containing 125 units of *HindIII* for 3 h at 37°C. For methylation detection, an aliquot of the *HindIII*-digested DNA was digested under the same conditions with a CpG methylase-sensitive enzyme, *HpaII*. As a control reaction, an aliquot was also digested with *MspI*, which is a CpG methylase-insensitive isoschizomer of *HpaII*. After ethanol precipitation, the digested DNA was loaded onto a 0.8% agarose gel in 0.1× Tris-borate-EDTA buffer for electrophoresis. After denaturation and the subsequent neutralization steps, the DNA was transferred to a positively charged nylon membrane (Roche Diagnostics). The filter was prehybridized for 1 h in DIG Easy Hyb buffer (Roche

**Table 2. Information on All the Patients with XDP Who Were Studied by Expression Analysis**

Patient Number	Age (years)		Clinical Description	Cause of Death	Fixation	Examination(s)*
	At Onset	At Death				
1 <sup>b</sup>	42	52	Dystonia and parkinsonism	Pneumonia	Frozen; 4% paraformaldehyde	NB, LRT, QRT, ISH
2	40	54	Dystonia and parkinsonism	Pneumonia	Formalin	IHC
3	23	47	Dystonia and parkinsonism	Pneumonia	Formalin	IHC
4	56	59	Dystonia	Suicide	Formalin	IHC
5	38	52	Dystonia	Unknown	Formalin	IHC
6	35	42	Dystonia	Suicide	Formalin	IHC
7	34	46	Dystonia	Pneumonia	Formalin	IHC

NOTE.—All patients are male.

\* IHC = immunohistochemical staining; ISH = in situ hybridization; LRT = long RT-PCR; NB = northern blot; QRT = quantitative RT-PCR.

<sup>b</sup> The results for patient 1 are presented in figures 2, 4, 5a-5e, 6, and 7.

**Table 3. PCR Primer Sets for Fragment Amplification from the *TAF1* cDNAs**

Fragment Name	Forward Primer			Reverse Primer			Amplicon Size (bp)
	Name <sup>a</sup>	Sequence (5'→3')	T <sub>m</sub> <sup>b</sup>	Name <sup>a</sup>	Sequence (5'→3')	T <sub>m</sub> <sup>b</sup>	
TA01	TAF_f_3	GGGAGCTCAGTAFAGTCACTTCTG	60.6	TAF_r_400	CCACCTCATTGATGTCGTAATAG	59.6	398
TA02	TAF_f_377	ACTAFTTCAGACATCAATGAGGTGG	60.4	TAF_r_772	TGGCATCATGCTGCATAATC	61.8	396
TA03	TAF_f_755	TFAFTGACGATGATGCCAC	60.4	TAF_r_1175	CCCAGCATATCACCACAGTC	60.4	421
TA04	TAF_f_1152	CCGACTGTGGTAFATGATAFTGCTG	61.5	TAF_r_1550	CGTCCATATACCAGATCTCATTG	62.7	399
TA05	TAF_f_1528	AATGAGGATCTGGTAFATGAGCG	60.2	TAF_r_1910	CGTAATCCACAGCAGGAATTG	62.7	383
TA06	TAF_f_1889	CAATTCCTGCTGGAAATFAFCG	62.7	TAF_r_2273	CCATATTTACAATCTGGTGTCTCC	60.7	385
TA07	TAF_f_2251	GGAGCACCAGATTGTAFAATAFTGG	60.7	TAF_r_2598	TTCCATTCGTATCCTCCGTG	62	348
TA08	TAF_f_2580	ACGGAGGATAFCGAATGGAAG	60.1	TAF_r_2979	ATCTGCCACCCAGTCAC	60.8	400
TA09	TAF_f_2945	GCAAGTGTCTGCTAFGAGGTGAC	60.3	TAF_r_3331	GTAGGTCAAAGATGCGCTGAC	61	387
TA10	TAF_f_3311	GTCAGCGCATCTTTGACCTAFC	61	TAF_r_3710	GTCCGTATGCGCACATAGG	61.3	400
TA11	TAF_f_3689	ATGCCTAFTGTGCGCATAFCG	61.8	TAF_r_4089	CAAGACAATTTGGTCCCTTC	59.6	401
TA12	TAF_f_4069	GAAGGGACCAAAATGTCCTTG	59.6	TAF_r_4467	TAGCTCCAGATGCTCTCTGAAC	59.9	399
TA13	TAF_f_4413	CGTGCGTAAACGCCCTCTAFC	60.6	TAF_r_4808	CGACTCTGATACTTGTGCTTGG	61	396
TA14	TAF_f_4780	AACATCTCCAAGCACAAAGTAFTCAG	60.7	TAF_r_5164	GCTTTTCTGGAGTGGCAGCTG	62.1	385
TA15	TAF_f_5130	TGCTTGGATAFTTCCAGTGC	61.1	TAF_r_5505	GTTGTATCCTCAAACCATG	60.5	376
TA16	TAF_f_5482	TCCCATGGTTTGGAGGATAFG	60.9	TAF_r_5862	AAGGCTAAGGTGTAGTTAATTCATG	60.3	381
TA17	TAF_f_5834	ATCATGAAATTAFACTAFACACCTTAFGCC	60.1	TAF_r_6231	TTAGTAGAGATGCGGTTTCGC	60.5	398
TA18	TAF_f_6073	GTAFACTTAFTGTCTCTTGTATGTAFTAFGG	59.1	TAF_r_6469	CAGGAGGGCTCTCATCTGC	62.3	397
TA19	TAF_f_6451	GCAGATGAGAGCCCTCCTG	62.3	TAF_r_6855	AAGGATCTGATAGAGTCTTATCATG	60.2	405
TA20	TAF_f_6831	ATGATAFAGCACTTAFTCAGATCCTTG	60.2	TAF_r_7164	CACACTCTGCCATTTAGACTG	60.1	334
TA21	TAF_f_7140	CACAGTCTAFGAAATGGCAGAGTG	60.1	TAF_r_7553	GGGTTATCATTGTGAACAGTTAGC	59.9	414
TA22	TAF_f_7277	GGCAGGAAGTAFTATCATCAACAAGC	62.1	TAF_r_7606	CCAGCATACATAACAACACAGAAG	60.9	330
MT23 <sup>c</sup>	TAF_f_7277	GGCAGGAAGTAFTATCATCAACAAGC	62.1	pMTS-r	GTGAGAGCTCAAAGACCAATAAG	58.3	779
Probe 1	TA_f_2333	TGCAAGCATTTGAGAAACAACCT	62	TA_r_2690	GAGTCCATCCTGTGCGCT	61.1	358
Probe 2	TA_f_4786	TCCAAGCACAAGTATCAGAGTCTG	61.7	TA_r_5185	CTTCACTTCTGTGTACCTGCT	63	400
Probe 3	TA_f_5637	GAGCGTACTAAGCCAGGTCCA	61.7	TA_r_6065	TTCATAATTTCCCTCCTTCCC	62.4	393

NOTE—The PCR mixture contained 2 μl of the first-strand cDNA, 0.2 mM of each dNTP, 1 μM of each primer, 1 × GeneAmp PCR buffer, and 2.5 units of AmpliTaq Gold DNA polymerase, in a 50-μl total volume. The PCR conditions were 9 min at 95°C, followed by 35 cycles at 95°C for 45 s, 60°C for 45 s, and 72°C for 60 s.

<sup>a</sup> The value in the third part of the primer name represents position in a major form of the *TAF1* transcript.

<sup>b</sup> T<sub>m</sub> = annealing temperature (°C). The calculation conditions were 1,000 nM of each primer and 50 mM potassium ions.

<sup>c</sup> The primer set was used only for first-strand cDNA from *MTS*.

**Table 4. Primers and Probes for the TaqMan Expression Assay**

Assay Name	Primer Sequence (5'→3')		Reporter 1 Sequence <sup>a</sup> (5'→3')	Amplicon Size (bp)
	Forward	Reverse		
TAF1-5'	GACTGACGGTGCTTGGT	GTCTGAATAGTCCACAGCATCTTCT	ACCCACCCCTTCATCATT	70
TAF1-3'	ACCTTATTCTGGCCAAACAGTGTT	ACAATCTCTGGGCAGTCTTAGTAT	ACTCTCAGGTCCATTATAC	73
TA02-334	TGGGACCAATGAAGAAGGATAAGGA	ATTCTGAGTCAGAGGAACACTGAAGT	CCACTTTCTCACCAGTAATAG	81
TA08-269	CTCTCGCGTCACTTCAAACG	TTCTCATTTTCTTCTTGGAGCAA	CCATAGCCAGCATCCTGT	79
TA09-391	GTGGTGAAGGATCTCCTATGTGAA	ATCTGTCTCTGCACTGCTCTTCTC	CAGCAGAAGGTAGGATGATAA	105
TA09-693	TGCCAAGCACTTCTACGTAATTTG	TCCAACCTATACAAAGCCCTAGT	CACACTCACCTCTTCC	99
TA14-317	ACCTTATTCTGGCCAAACAGTGTT	CCTCCAAAGTCTTCTTTAGCA	TTGAGTCAAATGTTATCATACAT	97
TA14-389	GGAGATTGTGAACGTCTGTTACCA	TCCTTCTCAAGTTGAGTCAAATGTTTCA	CATACTACCTCAGTCAATGTC	73
TA14-391	CCCCAGGGCCCTACAC	CTGAGGGATGTTGGTATCATAAA	CCTCAGGCTAAGCCTC	64
TA14-407	GGGAGAGCTTTCTGGATGATGTA	ACAATCTCTGGGCAGTCTTAGTAT	CTGACTCTCAGGTCTGCACG	119
TA15-477	AGTGCCACTCCAGAAAAGCA	CCTGCCAGCCTACT	CCTGGCGCATCTGTGT	61
TA18-261	GTGGCTCACACCTGTAATCTCA	CCTCCCGGGTCAAGTAATCTC	CAGCCTCCAGAGTGC	67
TA14-385N <sup>b</sup>	CCCCAGGGCCCTACAC	CTGAGGGATGTTGGTATCATAAA	CCTCAGCCTCTGATT	58
TAF1-M	GCTAAAGCTCTGCGCTGACT	TTAAGCACCCACAGTTTGTAGT	CATCCCTGTGCGTTGA	60
TAF1-3'N	CCCAGTGCCACTCCAGAAA	CAGTTCTTCTCTTCACTGCAA	ACCTTCTGTGTTACTGTC	82
MTS-V4	TTGCTCTGGGCTCTGCATT	CTGGCACGGATTTCACTATCTT	ACTCCTTACAGGTACCAATGA	251
MTS-37/1	CCCATGGTTTGGAGGATAGCA	CATCTCTGAATGGCTTGTTCATTG	TCAGGTGATGAACCTCAATA	166
MTS-37/3	CCCATGGTTTGGAGGATAGCA	TCGTTGCTCCAGAGATCTTTGTG	ACATCAGGTACCAATGAAC	83
MTS-2/3	GGCTCCGGCATTGCT	TCGTTGCTCCAGAGATCTTTGTG	TCCACTGTACCAATGAA	112
MTS-32'/34'	CAACAGTGTAAAGTATAATGGGTACATGTG	CTGAGGGATGTTGGTATCATAAA	TCAGGCTAAGCCTCTCT	268
MTS-3/4	GTGTCGGAGTTGGTCTCT	TGGCACGGATTTCACTATCTTCA	CCTTCGCGCTTCAGGC	105

<sup>a</sup> For the reporter 1 sequences, the dye was FAM.

<sup>b</sup> This probe is designed to detect all isoform sequences not containing exon 34'.

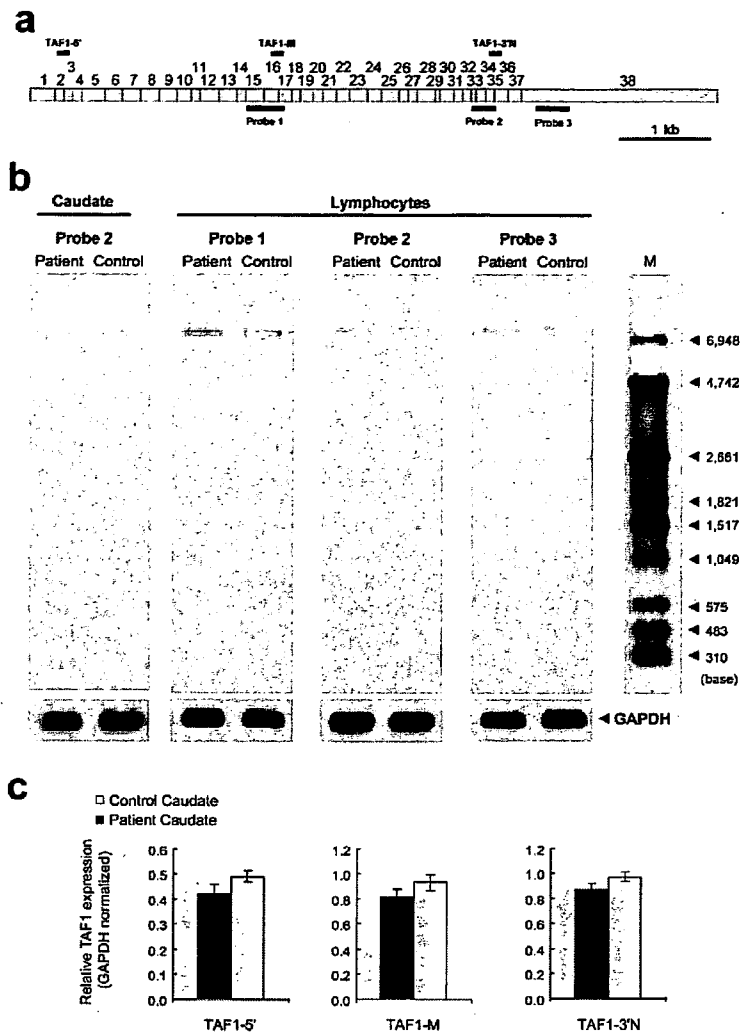


**Figure 2.** Northern analysis. *a*, Three probes for northern hybridization to *TAF1* (detailed information on these probes is given in table 3). *b*, Total RNA samples from the caudate and lymphoblastoid tissues. The hybridization signal seen at ~7 kb, which represents *TAF1*, was observed in every lane, but a signal was never seen at the smaller sizes corresponding to *MTS* transcripts reported elsewhere. This result suggests that the sequences of *TAF1* isoforms have such small differences in size, probably less than a few hundred base pairs, that standard northern analysis cannot discriminate between them in 1% agarose gels denatured by 2% formaldehyde. A probe for *GAPDH* was also hybridized to each membrane as a loading control. M = DIG-labeled molecular-weight marker. *c*, Relative *TAF1* expression. The hybridization signal seen at ~7 kb, representing *TAF1*, had a tendency toward slight reduction in patient caudate, so, to confirm this, TaqMan assays were performed.

Diagnostics) and then was hybridized overnight (16–18 h) at 40°C. The PCR probe was amplified using primers XD\_probe-F (5'-AGCTTTGCTGCCATTG-3') and XD\_probe-R (5'-AAGACCCTT-ATTATTCATGAGTG-3'). After washing the filter for 30 min at 68°C in DIG Wash and Block buffer, drops of 1/100-diluted disodium 3-(4-methoxy)spiro [1,2-dioxetane-3,2'-(5'-chloro) tricyclo

[3.3.1.1<sup>3,7</sup>]decan]-4-yl) phenyl phosphate (CSPD [Roche Diagnostics]) were added and the filter was exposed to x-ray film for 1–5 h.

#### RNA Isolation

Total RNA was isolated from caudate, cortex, and accumbens of a frozen brain by use of an RNeasy Lipid Tissue Midi kit (QIAGEN) with a DNaseI treatment step, after homogenization with a Polytron PT1300D (Kinematica). Total RNA from lymphoblastoid cell lines was also isolated by the same procedure. RNA sources from six Japanese brains were used as neurologically healthy con-

**Table 5. All Nucleotide Variants in the *DYT3* Critical Region on Xq13.1**

The table is available in its entirety in the online edition of *The American Journal of Human Genetics*.

trols by the same procedure. Also, two commercial human brain RNA sources were used as controls—cerebral cortex total RNA (catalog number 636561) and caudate nucleus total RNA (63566)—along with human tissue total RNA sources from heart (64100), spleen (64093), lung (64092), liver (64099), and thymus (64107), provided by BD Bioscience Clontech, and stomach (735038), provided by Stratagene. The quality and quantity of total RNAs were assessed using an Agilent 2100 Bioanalyzer (Agilent). The 2:1 ratio of 28S:18S rRNA was employed as a threshold for intact RNA. The quantity was confirmed by the RiboGreen RNA fluorescence assay (Molecular Probes).

#### Northern Analysis

For synthesis of riboprobes, we performed PCR and cloning into the TA-vector (Promega), using the three primer sets in table 3: TA\_f\_2333 and TA\_r\_2690 for probe 1, TA\_f\_4786 and TA\_r\_5185 for probe 2, and TA\_f\_5637 and TA\_r\_6065 for probe 3. Total RNA samples of 10  $\mu$ g were loaded into a 1% agarose gel denatured by 2% formaldehyde gel. The gel was run in  $1 \times 3$ [N-Morpholino]propanesulfonic acid buffer. After electrophoresis, the RNA was transferred to a positively charged nylon membrane. After prehybridization for 1 h in DIG Easy Hyb buffer at 68°C, hybridization was performed overnight (16–18 h) at 68°C. The filters were washed twice for 5 min with 100 ml of  $2 \times$  saline sodium citrate (SSC) and 0.1% SDS at room temperature and then were washed twice for 15 min with  $0.1 \times$  SSC and 0.1% SDS at 68°C. We employed the standard conditions and procedure provided by Roche Diagnostics.

#### Long RT-PCR Analysis

Long RT-PCR analysis was performed in two steps: (1) first-strand synthesis from RNAs of the control and XDP caudates by long reverse transcription (RT) and (2) fragment PCR by use of the long RT products (i.e., cDNA) as a template. Such a long RT-PCR method is known to be effective for defining the extent of a large transcript.<sup>11</sup> The two parts revealed not only the extent of the transcripts but also alternative exons included in the transcripts. Long RT was performed using TAF\_r\_7621 for the TATA-binding protein-associated factor 1 gene (*TAF1* [MIM 313650]) and MTS\_r for *MTS* as the long RT primer.

#### Quantitative RT-PCR

cDNA was synthesized from the total RNA by use of random hexamers with a TaqMan Reverse Transcription Reagents kit (Applied Biosystems). All the primers and probes are listed in table 4. We also employed a control probe for 18S rRNA (4319413E) and the glyceraldehyde-3-phosphate dehydrogenase gene (*GAPDH*) (4310884E) and examined a probe for the dopamine receptor D2 gene (*DRD2*) (Hs00156514\_m1). We used a final concentration of 250 nM probe, 900 nM primers, and 50 ng cDNA in a 50- $\mu$ l reaction volume in a 96-well reaction plate on an ABI PRISM 7000 in accordance with the standard procedure. The conditions of real-time PCR consisted of a holding step for 2 min at 50°C and 1 min at 95°C followed by 50 cycles for 15 s at 95°C and 1 min at 60°C. Quantity was calculated every time by use of a standard curve for each well. All quantitative data normalized by adjustment for 18S rRNA were tested by Smirnov's test with

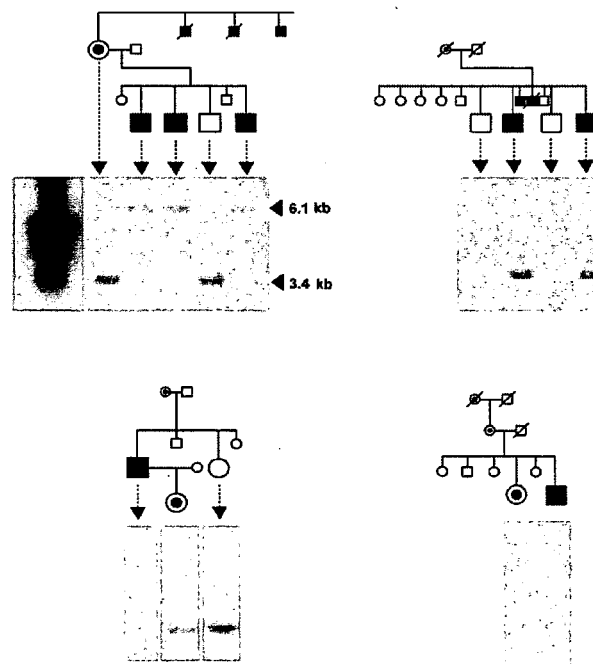


**Figure 3.** The SVA insertion in an additional seven patients with XDP and their relatives, from four families. Information on these patients is given in table 1 (patients 14–20).

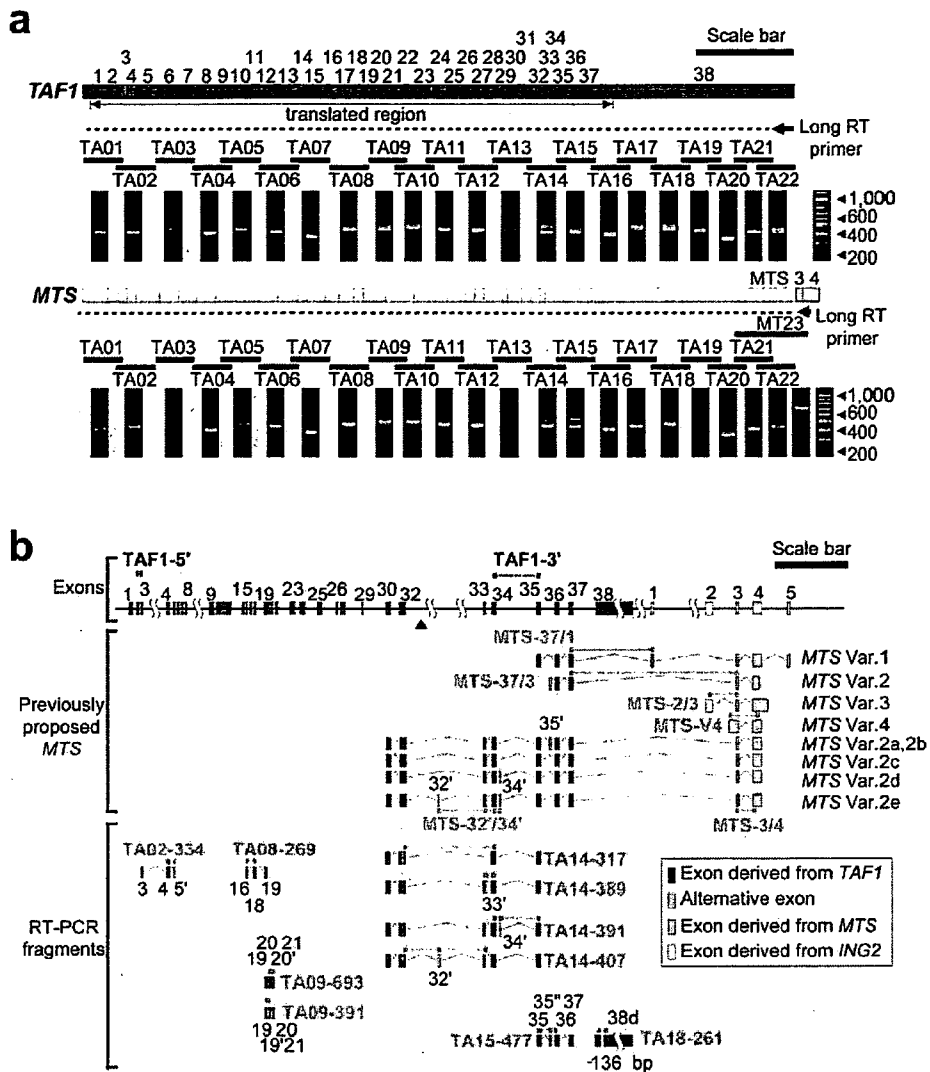


**Figure 4.** Long RT-PCR and the alternative exons of *TAF1*. *a*, Long RT-PCR analysis. The broken line indicates an expected cDNA fragment of *TAF1* with the long RT primer on the end of exon 38 (short arrow). By subsequent PCR with the use of the long cDNA, six lanes—TA02, TA08, TA09, TA14, TA15, and TA18 (red bars)—showed multiple bands. Other lanes (black bars) contained single bands. Also shown is the result obtained using the *MTS*-specific long RT primer on its 3' end. There was no difference between the *TAF1* and *MTS* primers or between the patient and the control results (patient data not shown). Scale bar = 1 kb. *b*, Ten alternative exons, including two exon skipplings and one deletion, were identified by RT-PCR. The detailed sequence information for these exons is annotated in our AB191243 deposition in DNA Databank of Japan (DDBJ). Of 10 alternative exons, 3 were reported elsewhere as exons of *MTS*, but a form including both exon 32' and exon 34' was not detected. For quantitative RT-PCR, 17 TaqMan probes were designed. Two TAF-series probes (red) and 10 TA-series probes (pink) were designed to detect mainly the *TAF1* common forms and alternative splicing isoforms, respectively. The other five *MTS*-series probes (orange) were designed to detect the *MTS* transcripts reported elsewhere. Var. = variant. Scale bar = 5 kb.

a 5% significance level. We used Student's *t* test to test the difference in means of the expression levels between patients with XDP and healthy control caudate nuclei, after checking the acceptance of the quality of variances between the two groups by the *F* test.

#### *In Situ Hybridization*

Synthesis of DIG-labeled riboprobes for *TAF1* (probe 3 in fig. 2a), as well as for  $\beta$ -actin (*ACTB*) and glial fibrillary acidic protein (*GFAP*) as controls, was performed according to the procedure

**Table 6. Linearity of Amplification Curve from Threshold Cycle (Ct) = 25 to Ct = 35**

Assay	Slope (SD)	r (SD)	r <sup>2</sup> (SD)
MTS-37/1	.0020 (.0032)	.31 (.641)	.48 (.226)
MTS-37/3	.035 (.0123)	.82 (.036)	.68 (.061)
MTS-V4	.011 (.0098)	.51 (.422)	.43 (.285)
MTS-2/3	.00016 (.0014)	-.10 (.580)	.32 (.213)
MTS-32/34 <sup>a</sup>	.00073 (.0005)	.77 (.258)	.65 (.292)
MTS-3/4	.054 (.0351)	.81 (.017)	.66 (.032)
TA14-385N <sup>a</sup>	1.37 (.0424)	.99 (.002)	.97 (.004)

NOTE.—Slopes of the resulting lines, correlation coefficient (*r*) values, and coefficient of determination (*r*<sup>2</sup>) values were calculated by curve-fitting with linear function against normalized reporter signal ( $\Delta Rn$ ) values from Ct = 25 to Ct = 35 in each amplification curve of the real-time PCRs. We employed the threshold with slope >0.5 and *r*<sup>2</sup> > 0.6.

<sup>a</sup> The TaqMan probe was employed as a positive control to show standard amplification and linearity from Ct = 25 to Ct = 35.

used for northern analysis. The caudate blocks were fixed with 4% paraformaldehyde. After cryoprotection, serial 20- $\mu$ m sections were cut in a cryostat. The sections were reacted with alkaline phosphatase-labeled anti-DIG antibody (diluted 1:200 [Roche Diagnostics]) in 1% skim milk in sodium Tris (hydroxymethyl)-ammonium buffer (NT) buffer. After washing with NT buffer, the positive signals were detected by nitroblue tetrazolium chloride (Roche Diagnostics) and 187  $\mu$ g/ml 5-bromo-4-chloro-3-indolylphosphate (Roche Diagnostics).

#### Immunohistochemical Staining

The six tissues from six different patients with XDP were fixed in 10% neutral formalin, were sliced, and were embedded in paraffin, and 3- $\mu$ m sections were cut on a microtome and were mounted on Matsunami adhesive silane-coated glass slides. After routine deparaffinization, rehydration, and blocking of endogenous peroxidase activity, all sections were processed for microwave-enhanced antigen retrieval. The sections were blocked with 3% BSA in PBS (pH 7.2) for 1 h and then were incubated overnight at room temperature in 3% BSA-PBS containing goat polyclonal antibody against *TAF1* (diluted 1:5,000 [Santa Cruz]). Rabbit polyclonal antibody against *GFAP* (Dako) was also used as a control. For the visualization of bound antibodies, we used Histofast Simplestain Max-PO (G) (Nichirei) and the liquid diaminobenzidine (DAB) substrate chromogen system (Dako Cytomation). The sections were further processed for enhancement of the DAB reaction products by use of a Dako Envision Kit (Dako Cytomation).

#### Full-Length Cloning and Direct Sequencing of the TA14\_391 Isoform

To determine the full-length *TAF1* isoform, including the 5' end of the transcript, a CapSite cDNA library derived from human brain (317-04041 [Nippon Gene]) was used. The CapSite cDNA libraries consist of cDNAs in which the 5' cap structure (m<sup>7</sup>Gppp) of eukaryotic mRNA is replaced with a synthetic oligoribonucleotide to label the 5' end of the cDNA, enabling identification of the 5' end sequence by PCR.<sup>10</sup> For amplification of the 3' end, a whole Marathon-Ready cDNA library derived from human brain (BD Biosciences Clontech) was used. The reaction mixture contained 1  $\mu$ l of the library, 200 mM of each primer, 0.16 mM of each deoxyribonucleotide diphosphate (dNTP), 1  $\times$  BD Advantage2 PCR buffer, and 1  $\times$  BD Advantage2 Polymerase Mix

(639300 [BD Biosciences Clontech]) in a total volume of 50  $\mu$ l. The PCR consisted of denaturation for 30 s at 94°C, followed by 5 cycles for 5 s at 94°C and 10 min at 70°C and then 20 cycles for 5 s at 94°C and 10 min at 78°C. An aliquot of the first PCR product was used for the second PCR reaction under the same conditions as the first-round PCR but with different primers. We used a primer set for the first PCR—first RDT primer (Nippon Gene) and TA3\_r\_5070 (5'-GGTATCATACAAATCAGGAGGCTT-3')—and then used a set for the second heminested PCR—second primer and TA3\_r\_5070. These primers were purified by PAGE extraction. Alternative exon 34'-specific primers were designed to prevent erroneous amplification due to PCR slippage. For amplification of the 3' end, a whole Marathon-Ready cDNA library derived from human brain (BD Biosciences Clontech) was used along with the primer set TA6\_f\_5032 (5'-CCCTACACGCCTCAG-GCTA-3') and TA2\_r\_7606 (5'-CCAGCATACATAACAACACAG-AAG-3') under the same conditions as those used for the CapSite cDNA but as a single PCR reaction. Direct sequencing was done on these PCR products. After purification by a PCR Product Pre-Sequencing kit, cycle sequencing was performed using a BigDye Terminator v3.1 Cycle Sequencing kit, with 20 internal primers for a second PCR product from CapSite cDNA and 8 internal primers for the PCR product from Marathon-Ready cDNA. Direct sequencing was done on two long PCR products by use of the following primers: TAF\_f\_377, TAF\_f\_755, TAF\_f\_1152, TAF\_f\_1528, TAF\_f\_1889, TAF\_f\_2580, TAF\_f\_2945, TAF\_f\_3311, TAF\_f\_3689, TAF\_f\_4069, TAF\_f\_4413, TAF\_f\_4780, TAF\_r\_2273, TAF\_r\_2598, TAF\_r\_2979, TAF\_r\_3331, TAF\_r\_5164, TAF\_r\_5505, TAF\_r\_5862, TAF\_r\_6231, TAF\_r\_6469, TAF\_r\_6855, TAF\_r\_7164, TAF\_r\_7553, and TAF\_r\_7606 (table 3).

## Results

### Entire Genomic Sequence of the DYT3 Region

Two series of BAC libraries were constructed using DNA from a patient with XDP who had a disease-specific haplotype<sup>8,9</sup> in the *DYT3* region. From these libraries, a continuous BAC contig consisting of eight BAC clones was then generated to cover the *DYT3* region between the *GJB1* and *CXCR3* genes (fig. 1a). By applying a shotgun sequencing strategy, we accurately determined the complete DNA sequence of the BAC contig, with 5.7-fold redundancy. The total sequence length of the BAC contig was 463,567 bp. A comparison between our sequence from the patient with XDP and a reference sequence from National Center for Biotechnology Information (NCBI) build 30 showed a total of 159 sequence variants: 89 single-nucleotide substitutions, 68 small insertions/deletions (indels), 1 retrotransposal insertion, and 1 large (1,666-bp) deletion (all variants are listed in table 5). Of these variants, 53 were known SNPs, comprising 50 substitutions and 3 indels. Of the 68 indels, 62 were repetitive units of STRs, and the other 6 indels were also located in certain types of STRs. The large deletion was a direct repeat sequence spanning 1,666 bp. The retrotransposal insertion in intron 32 of the *TAF1* gene (fig. 1a) was 2,627 bp in length, which is categorized as an SVA (short interspersed nuclear element, VNTR, and Alu composite) retrotransposon.<sup>12,13</sup> The SVA retrotransposon insertion in the *DYT3* region had been never reported. However, none of these

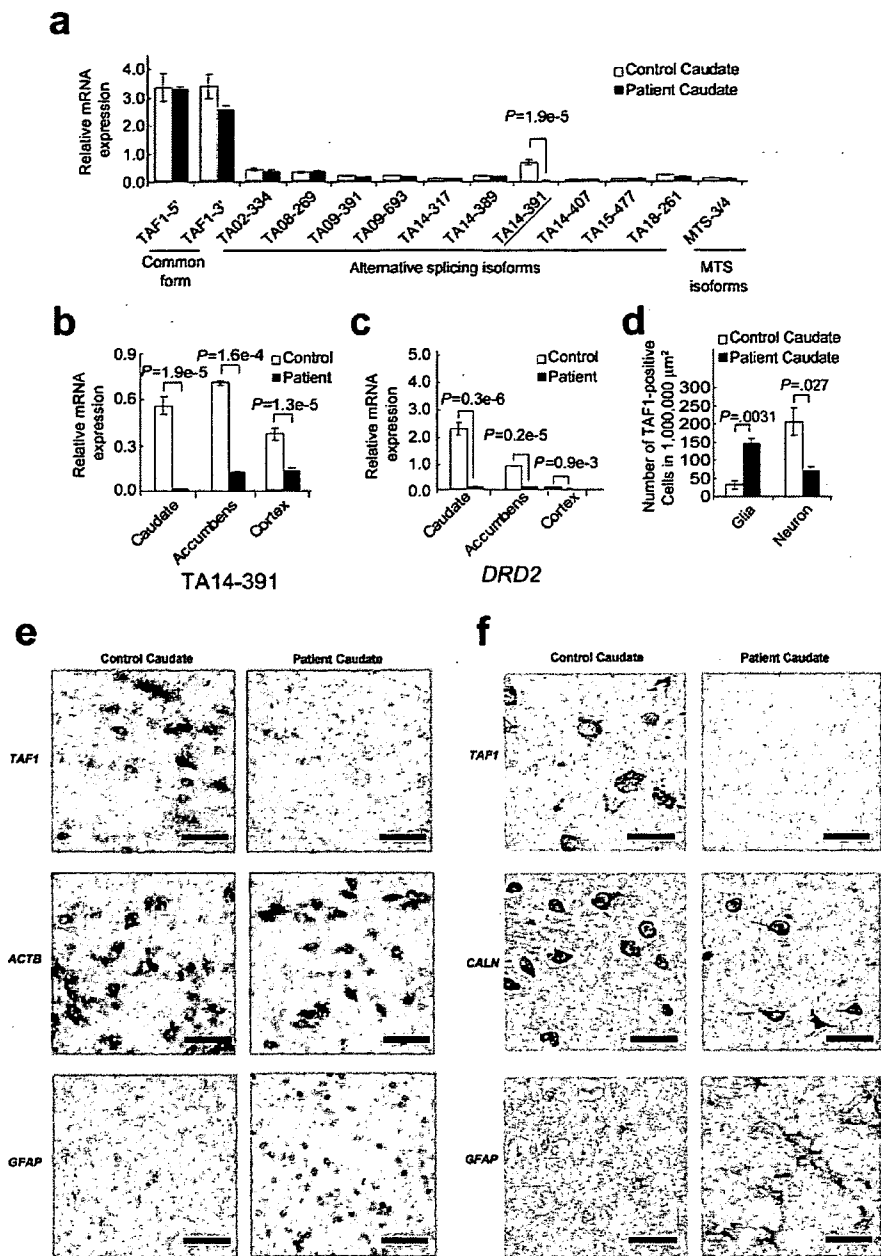


**Figure 5.** Expression of the TAF1 isoforms in the caudate. *a*, Expressions are shown relative to the expression of 18S rRNA (as an internal control). The label "relative mRNA expression" means relative mRNA expression level to  $1/20 \times 18S$  rRNA. Values are expressed as means  $\pm$  SEM ( $n = 3$ ). The TA14-391 probe showed a significant reduction in the patient's caudate. Two-sided  $P$  values are shown. Also shown is the expression level of TA14-391 (*b*) and *DRD2* (*c*) in three brain regions: caudate, accumbens, and cortex. All regions showed a significant decrease in TA14-391 expression. *d*, Morphometry analysis of TAF1-positive cells in XDP and control caudate nuclei. The number of each type of cell was counted in 1,000,000- $\mu\text{m}^2$  areas of the caudate nuclei. These were gliosis and neuronal loss in the XDP caudate nucleus. *e*, In situ hybridization analysis of TAF1. Although many TAF1-positive neurons were observed in both tissues, the expression level was apparently low in the patient's caudate neurons, even when a common probe for exon 38 was used. By contrast, the expression level of TAF1 in glial cells was weak in both tissues. ACTB =  $\beta$ -actin; GFAP = glial fibrillary acidic protein. Strong ACTB signals were shown in glial and neuronal cells. The GFAP probe stains active glial cells, especially in the XDP caudate nucleus, because of activation by astroglia. In contrast, we observed no signal when using sense probes of these genes (data not shown). Scale bar = 25  $\mu\text{m}$ . *f*, TAF1 immunohistochemical staining. Nearby sections were stained with polyclonal antibodies against TAF1, calcineurin (CALN), and GFAP. The immunoreactivity of TAF1 in the XDP caudate neurons was apparently weak. Moreover, the immunoreactivity of TAF1 in glial cells was originally weak in both tissues. Similar immunoreactivity was observed in three other brain tissues from three different patients with XDP. Scale bar = 25  $\mu\text{m}$ .



**Table 7. Abundance of the Probe TA14-391 in Various Tissues and Cell Lines**

Tissue or Cell Line	Mean (SE) [10 <sup>-5</sup> fmol per 100 ng RNA]	
	TA14-391	TAF1 Major Form
Lymphocytes	0	3.68 (.08897)
Heart	0	.0873 (.00484)
Spleen	0	3.13 (.06749)
Lung	0	.133 (.00536)
Liver	0	4.20 (.21582)
Thymus	0	1.44 (.07147)
Stomach	0	1.23 (.03865)
Caudate	.699 (.00761)	3.30 (.50351)
Cortex	.463 (.00308)	3.70 (.57268)
Neuroblastoma, SH-SY5Y	.213 (.00694)	4.68 (.55110)
Glioblastoma, HTB15	0	1.67 (.44595)

NOTE.—The abundances for TA14-391 and the TAF1 major form (TA14-385N) were determined using quantitative RT-PCR by use of each clone of known concentration in the plasmid as an internal control.

variants was located in any exon or promoter of the annotated genes that have experimentally verified coding sequences, including their alternative splicing exons. In the region between *DXS10017* and *DXS10018*, there were 25 variants, which included the SVA insertion and the 1,666-bp deletion. We confirmed these variants in an ethnic panel (see the “Material and Methods” section) that included patients with XDP who have the disease-specific haplotype. DSCs 12, 10, 1, 3, and 2 were disease-specific among patients with XDP tested here as well as in a previous report.<sup>9</sup> The 1,666-bp deletion was detected by PCR among all affected and unaffected Filipinos and in the ethnic panels (data not shown) and was considered to be nonspecific. By contrast, the SVA retrotransposon was clearly disease specific in our data set (figs. 1*b* and 3). These disease-specific variants, the DSCs and the SVA retrotransposon, were located around the *TAF1* and *MTS* genes.

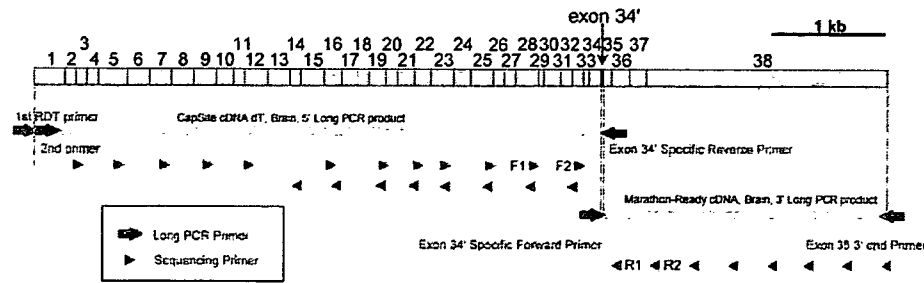
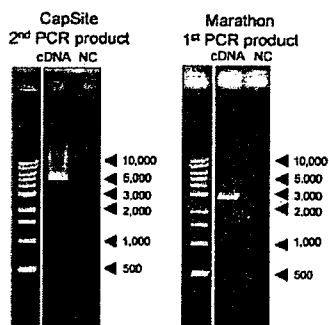
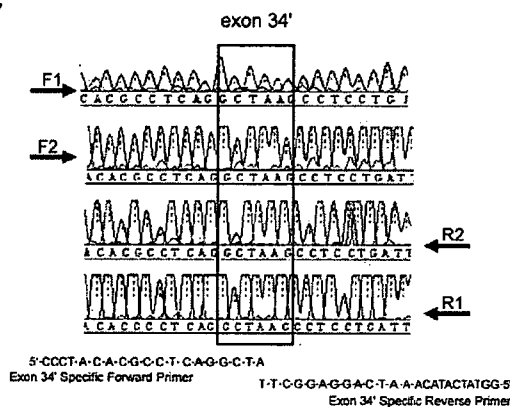
#### Previously Proposed *MTS* Transcripts

Next, northern hybridization and long RT-PCR analysis were undertaken to confirm the structures and expression of the *TAF1* and *MTS* genes. Northern analysis showed that the hybridization signal seen at ~7 kb of *TAF1* had a tendency toward reduction in patient caudate and that the *MTS* transcript lengths reported elsewhere<sup>9</sup> were not detectable in RNAs from either patient or control tissues (fig. 2*b*). Long RT-PCR analysis showed that the PCR fragment pattern from *MTS* was identical to that from *TAF1* (fig. 4*a*). If the *MTS* transcripts had lacked upstream exons 1–29 and exon 38, spanning >2 kb, as shown in the previous report,<sup>9</sup> the northern analysis would have detected the corresponding signals at ~2–5 kb. Moreover, our long RT-PCR analysis showed that exons 3 and 4 from *MTS* (gray exons in fig. 4*b*) are attached at the 3' end of exon 38 of *TAF1*. Quantitative RT-PCR analysis by the TaqMan assay with five probes designed to detect the previously proposed *MTS* transcripts *MTS-V4*—which was regarded

as a candidate transcript for *DYT3* because of a deduced amino-acid change<sup>9</sup>—*MTS-37/1*, *MTS-37/3*, *MTS-2/3*, and *MTS-32/34'* (fig. 4*b*) yielded very weak and irregular amplification signals that did not allow quantification of expression levels in the caudate nucleus (table 6), whereas the probe *MTS-3/4* for exons 3 and 4 attached to *TAF1* yielded a relatively weak but regular signal (table 6). These results consistently suggested that the previously proposed *MTS* transcripts may be extremely rare or unexpressed and that at least exons 3 and 4 of *MTS* may be just an additional part of the 3' UTR of *TAF1*, rather than part of a new distinct short gene.

#### Decreased Expression of TAF1 in the XDP Brain

At least 10 new alternative splicing exons around *TAF1* were found by long RT-PCR analysis (fig. 4*b*), but neither the DSCs nor the SVA insertion were located in any known and predictably translated regions of the *TAF1* exons. We then examined the expression levels of various forms of *TAF1* in the XDP caudate nucleus, using quantitative RT-PCR by designing specific probes for the TaqMan assay (fig. 5*a*). One of these probes, TA14-391—with an alternative exon of 6 additional bp, named “exon 34'”—showed a highly significant decrease in its expression level in the caudate nucleus of the patient with XDP (fig. 5*a*), which was less than ~1/40 of that in the normal control, and its expression was virtually limited to brain and neurons (table 7). TA14-391 was the second-most abundant among all *TAF1* species (fig. 5*a*), and its expression level in the control caudate nucleus was 1/4–1/5 of that of the major form of *TAF1* (table 7). TA14-391 also showed a significantly decreased level of expression in the cortex and the nucleus accumbens of the patient with XDP (fig. 5*b*), although these regions had no neuronal loss. These findings suggest that the decreased level of expression was the cause rather than the result of neuronal loss in the caudate nucleus of the patient with XDP. In addition to the TaqMan assay, *in situ* hybridization was performed in the caudate by use of a riboprobe common to TAF1 isoforms that are located in exon 38 (probe 3 in fig. 2*a*). The riboprobe showed decreased expression in the caudate neurons of the patient, although the weak expression was still present in glial cells (fig. 5*e*). Immunohistochemical examination by use of a polyclonal antibody against the common epitopes of *TAF1* also showed decreased immunoreactivity in the XDP neurons in the caudate nucleus from other patients with XDP (fig. 5*f*). These findings suggest that the deficiency of the neuron-specific isoform of TAF1, TA14-391, reflects these histologically verified neuron-specific decreases of *TAF1* expression and that TA14-391 is one of the neuron-specific isoforms, whereas apparently similar levels of mRNA expression for TAF1 or its isoforms as a whole (figs. 2*b*, 2*c*, and 5*a*) can be accounted for by increased glial expression of *TAF1* due to intensive astrogliosis<sup>4,5</sup> (fig. 5*d–5f*), obscuring the decreased expression in neurons. The TA14-391 isoform may

**a****b****c**

**Figure 6.** *a*, Full-length cloning of a TAF1 isoform sequence containing alternative exon 34'. The 5' end was obtained from CapSite cDNA from brain. The 3' end was obtained from Marathon-Ready cDNA from brain. The complete DNA sequences of these long products were determined by a PCR direct-sequencing method by use of 28 redundant internal sequencing primers (red triangles). *b*, From the long PCR products, products of sufficient quantity and quality for PCR direct sequencing were amplified. NC = negative control without DNA template. *c*, Each exon 34'-specific primer was designed to have only 3 nt of exon 34', to prevent erroneous amplification due to slippage.

represent the decreased expression of many TAF1 isoforms in the XDP neurons, because of its original neuron specificity of expression. Finally, to determine the complete structure of the isoform containing the 6 bp of exon 34', full-length cloning from libraries consisting of cDNAs enriched in their 5' ends<sup>10</sup> was performed. A single cDNA containing exon 34' was successfully cloned (fig. 6), and this had the complete translation frame of the major form of TAF1 with an insertion of two amino acid residues, alanine and lysine, in the carboxyl terminal kinase domain.

## Discussion

SVA retrotransposon insertions are thought to be active in the human genome and to alter the expression level of adjacent genes that cause diseases, such as autosomal recessive hypercholesterolemia (ARH [MIM 605747])<sup>14</sup> and Fukuyama-type congenital muscular dystrophy (FCMD

[MIM 607440]).<sup>15</sup> SVA insertion was found in the 3' UTR region of the FCMD gene and in an intronic region of the ARH gene, which showed association with the reduced expression level of these genes. SVA retrotransposon has a high degree of GC content (~70%) and a large number of CpG sites (>150) in its nucleotide sequence, so that it is frequently hypermethylated in its insertion site. In fact, the present study demonstrated that the SVA retrotransposon was hypermethylated in genomic DNA from the caudate nucleus of the patient with XDP (fig. 7), which was also used in northern analysis, quantitative RT-PCR, and in situ hybridization. Such hypermethylated status and high GC content are able to affect dynamics of surrounding nucleotide sequence, such as the *cis*-regulatory element, so SVA insertions may reduce the expression level of adjacent genes. For instance, many large introns of eukaryotes often contain tissue-specific *cis*-regulatory elements, such as enhancers or silencers.<sup>16-22</sup> Intron 32, the largest intron of TAF1 (29,932 bp), possibly contains a

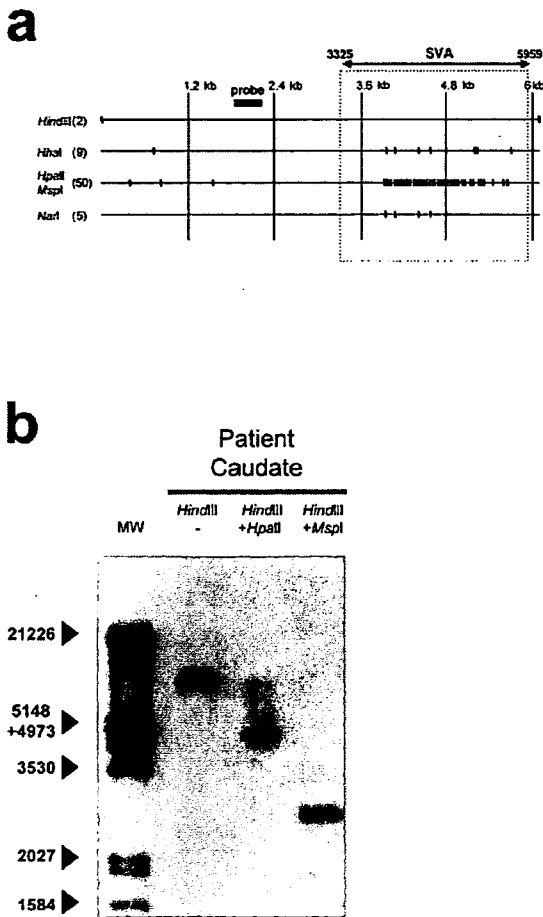


**Figure 7.** Detection of methylation around the SVA insertion. *a*, Restriction sites around the SVA insertion. The *Hind*III fragment and Southern probe are identical to those in figure 1*a*. The SVA insertion created 47 new *Hpa*II sites in the *Hind*III restriction fragment. *Msp*I is a CpG methylase-insensitive isoschizomer of *Hpa*II. *b*, Southern hybridization of genomic DNA from the patient's caudate. The 6.1-kb *Hind*III fragment was shifted, by additional *Hpa*II digestion, to an ~4.6-kb fragment. By contrast, the *Hind*III fragment was completely digested, by additional *Msp*I digestion, to a fragment of ~2.4 kb.

neuron-specific *cis*-regulatory element. Although involvement of other sequence variants in XDP pathogenesis is still possible, it is most likely that the SVA insertion impairs the function of a hypothetical neuron-specific *cis*-regulatory element, such as an enhancer, through changes in the methylation content and then substantially reduces the expressions of many isoforms of TAF1, including TA14-391, in the neurons. Because of the original neuron specificity of the expression, the TA14-391 isoform might represent the impairment more remarkably than do other isoforms. On the other hand, the remaining expression,

as shown for TA14-391, despite being low, may compensate for complete loss of function and may account for the relatively late disease onset (age  $39.5 \pm 8.44$  years) and the recessive mode of inheritance.

In summary, our results suggest that the SVA retrotransposon insertion into the *TAF1* gene may cause XDP by altering the expression of TAF1 isoforms, including TA14-391, possibly through DNA methylation changes. To our knowledge, our report is the first to reveal the entire genomic sequence of the *DYT3* region and to demonstrate at least one whole structure of the neuron-specific isoform of TAF1 and the disease-specific mutation, with a possible mechanism. To establish the disease specificity and the involvement mechanism of the SVA insertion in reduced expression of *TAF1* in XDP, further studies, such as an extensive population screening and genetic modification in model organisms, will be necessary and warranted. The TAF1 protein is the largest and the essential component of the TFIID complex in the pathway of RNA polymerase II-mediated gene transcription,<sup>23,24</sup> and it regulates transcription of a large number of genes related to cell division and proliferation.<sup>23-25</sup> How can a ubiquitous gene such as *TAF1* cause a disease that affects a selective part of the nervous system? We hypothesize that the neuron-specific isoforms and/or their enhanced expression level of *TAF1* (table 7) may play important roles in the nondividing cell. Sharing similar pathological features in the caudate nucleus, XDP and Huntington disease might result from disorders in the same biochemical pathway of RNA polymerase II-mediated gene transcription. In Huntington disease, for example, the abnormal huntingtin protein has been shown to interfere with the interaction between Sp1 and TAFII130, resulting in reduced expression of *DRD2* (MIM 126450) in the brain, including the caudate nucleus.<sup>26</sup> In XDP, the decreased expression of the TA14-391 isoform, and probably other TAF1 isoforms, may result in transcriptional dysregulation of many neuronal genes, including *DRD2*. We believe that the present findings in XDP support the concept of "transcription syndromes"<sup>27</sup> in TFIID, which include congenital cataracts facial dysmorphism neuropathy (CCFDN [MIM 604168]) syndrome, caused by a partial deficiency of RNA polymerase II<sup>28</sup>; Huntington disease<sup>26</sup>; dentato-rubro-pallidolusian atrophy (DRPLA [MIM 125370]),<sup>29</sup> caused by interference in the signals to TFIID; and spinocerebellar ataxia 17 (SCA17 [MIM 607136]),<sup>30</sup> caused by an expanded polyglutamine in the TATA-binding protein (TBP [MIM 600075]).

#### Acknowledgments

We thank S. Fahn (Neurological Institute of New York, Columbia University) and M. Nakagawa (Kyoto Prefectural University of Medicine) for their critical reading of the manuscript. This study was partly supported by a Grant-in-Aid for Scientific Research on Priority Areas (C) "Medical Genome Science"; by Center of Excellence grant 16101J-1 from the Japanese Ministry of Education,

Science, Culture, and Sports; and by Grant-in-Aid for Dystonia Research from the National Center of Neurology and Psychiatry, Japan.

### Web Resources

Accession numbers and URLs for data presented herein are as follows:

dbSNP, <http://www.ncbi.nlm.nih.gov/SNP/> (for newly described SNPs *ss66974122*, *ss66974125*, *ss66974128*, *ss66974131*, *ss66974134*, *ss66974137*, *ss66974140*, *ss66974143*, *ss66974146*, *ss66974149*, *ss66974152*, and *ss66974155*)

DNA Databank of Japan (DDBJ), <http://www.ddbj.nig.ac.jp/Welcome-e.html> (for the complete genomic sequence of the *DYT3* region [accession number AB191243])

Online Mendelian Inheritance in Man (OMIM), <http://www.ncbi.nlm.nih.gov/Omim/> (for XDP, Huntington disease, *TAF1*, *ARH*, *FCMD*, *DRD2*, *CCFDN*, *DRPLA*, *SCA17*, and *TBP*)

### References

1. Lee LV, Pascasio FM, Fuentes FD, Viterbo GH (1976) Torsion dystonia in Panay, Philippines. *Adv Neurol* 14:137–151
2. Lee LV, Munoz EL, Tan KT, Reyes MT (2001) Sex linked recessive dystonia parkinsonism of Panay, Philippines (XDP). *Mol Pathol* 54:362–368
3. Fahn S, Bressman SB, Marsden CD (1998) Classification of dystonia. *Adv Neurol* 78:1–10
4. Goto S, Lee LV, Munoz EL, Tooyama I, Tamiya G, Makino S, Ando S, Dantes MB, Yamada K, Matusmoto S, et al (2005) Functional anatomy of the basal ganglia in X-linked recessive dystonia-parkinsonism. *Ann Neurol* 58:7–17
5. Waters CH, Faust PL, Powers J, Vinters H, Moskowitz C, Nygaard T, Hunt AL, Fahn S (1993) Neuropathology of lubag (X-linked dystonia parkinsonism). *Mov Disord* 8:387–390
6. Wilhelmsen KC, Weeks DE, Nygaard TG, Moskowitz CB, Rosales RL, dela Paz DC, Sobrevega EE, Fahn S, Gilliam TC (1991) Genetic mapping of "Lubag" (X-linked dystonia-parkinsonism) in a Filipino kindred to the pericentromeric region of the X chromosome. *Ann Neurol* 29:124–131
7. Haberhausen G, Schmitt I, Kohler A, Peters U, Rider S, Chelly J, Terwilliger JD, Monaco AP, Muller U (1995) Assignment of the dystonia-parkinsonism syndrome locus, *DYT3*, to a small region within a 1.8-Mb YAC contig of Xq13.1. *Am J Hum Genet* 57:644–650
8. Nemeth AH, Nolte D, Dunne E, Niemann S, Kostrzewa M, Peters U, Fraser E, Bochukova E, Butler R, Brown J, et al (1999) Refined linkage disequilibrium and physical mapping of the gene locus for X-linked dystonia-parkinsonism (*DYT3*). *Genomics* 60:320–329
9. Nolte D, Niemann S, Muller U (2003) Specific sequence changes in multiple transcript system *DYT3* are associated with X-linked dystonia parkinsonism. *Proc Natl Acad Sci USA* 100:10347–10352
10. Maruyama K, Sugano S (1994) Oligo-capping: a simple method to replace the cap structure of eukaryotic mRNAs with oligoribonucleotides. *Gene* 138:171–174
11. Lee JT, Davidow LS, Warshawsky D (1999) Tsix, a gene antisense to Xist at the X-inactivation centre. *Nat Genet* 21:400–404
12. Shen L, Wu LC, Sanlioglu S, Chen R, Mendoza AR, Dangel AW, Carroll MC, Zipf WB, Yu CY (1994) Structure and genetics of the partially duplicated gene *RP* located immediately upstream of the complement *C4A* and the *C4B* genes in the HLA class III region: molecular cloning, exon-intron structure, composite retroposon, and breakpoint of gene duplication. *J Biol Chem* 269:8466–8476
13. Ostertag EM, Goodier JL, Zhang Y, Kazazian HH Jr (2003) SVA elements are nonautonomous retrotransposons that cause disease in humans. *Am J Hum Genet* 73:1444–1451
14. Wilund KR, Yi M, Campagna F, Arca M, Zuliani G, Fellin R, Ho YK, Garcia JV, Hobbs HH, Cohen JC (2002) Molecular mechanisms of autosomal recessive hypercholesterolemia. *Hum Mol Genet* 11:3019–3030
15. Kobayashi K, Nakahori Y, Miyake M, Matsumura K, Kondoiida E, Nomura Y, Segawa M, Yoshioka M, Saito K, Osawa M, et al (1998) An ancient retrotransposal insertion causes Fukuyama-type congenital muscular dystrophy. *Nature* 394:388–392
16. Gillies SD, Morrison SL, Oi VT, Tonegawa S (1983) A tissue-specific transcription enhancer element is located in the major intron of a rearranged immunoglobulin heavy chain gene. *Cell* 33:717–728
17. Halder G, Callaerts P, Gehring WJ (1995) Induction of ectopic eyes by targeted expression of the eyeless gene in *Drosophila*. *Science* 267:1788–1792
18. Dirksen WP, Mohamed SA, Fisher SA (2003) Splicing of a myosin phosphatase targeting subunit 1 alternative exon is regulated by intronic cis-elements and a novel bipartite exonic enhancer/silencer element. *J Biol Chem* 278:9722–9732
19. Donoghue M, Ernst H, Wentworth B, Nadal-Ginard B, Rosenthal N (1988) A muscle-specific enhancer is located at the 3' end of the myosin light-chain 1/3 gene locus. *Genes Dev* 2:1779–1790
20. Annweiler A, Muller-Immergluck M, Wirth T (1992) Oct2 transactivation from a remote enhancer position requires a B-cell-restricted activity. *Mol Cell Biol* 12:3107–3116
21. Banerji J, Rusconi S, Schaffner W (1981) Expression of a beta-globin gene is enhanced by remote SV40 DNA sequences. *Cell* 27:299–308
22. Rippe RA, Lorenzen SJ, Brenner DA, Breindl M (1989) Regulatory elements in the 5'-flanking region and the first intron contribute to transcriptional control of the mouse alpha 1 type I collagen gene. *Mol Cell Biol* 9:2224–2227
23. Hisatake K, Hasegawa S, Takada R, Nakatani Y, Horikoshi M, Roeder RG (1993) The p250 subunit of native TATA box-binding factor TFIID is the cell-cycle regulatory protein CCG1. *Nature* 362:179–181
24. Ruppert S, Wang EH, Tjian R (1993) Cloning and expression of human TAFII250: a TBP-associated factor implicated in cell-cycle regulation. *Nature* 362:175–179
25. Wassarman DA, Sauer F (2001) TAF(II)250: a transcription toolbox. *J Cell Sci* 114:2895–2902
26. Dunah AW, Jeong H, Griffin A, Kim YM, Standaert DG, Hersch SM, Mouradian MM, Young AB, Tanese N, Krainc D (2002) Sp1 and TAFII130 transcriptional activity disrupted in early Huntington's disease. *Science* 296:2238–2243
27. Vermeulen W, van Vuuren AJ, Chipoulet M, Schaeffer L, Appeldoorn E, Weeda G, Jaspers NG, Priestley A, Arlett CF, Lehmann AR, et al (1994) Three unusual repair deficiencies associated with transcription factor BTF2(TFIIF): evidence for the existence of a transcription syndrome. *Cold Spring Harb Symp Quant Biol* 59:317–329
28. Varon R, Gooding R, Steglich C, Marns L, Tang H, Angelicheva